International Journal of Earth Sciences (2023) 112:1389–1412
https://doi.org/10.1007/s00531-023-02311-8

ORIGINAL PAPER

Geochemical fingerprint—inter-basin chemostratigraphic correlation allowed for a more detailed stratigraphic subdivision of the Pliensbachian–Bathonian strata from the Carpathian Foredeep basement (Ukraine)

Adam Zakrzewski[1] · **Marcin Krajewski**[1] · **Paweł Kosakowski**[1]

Received: 13 February 2023 / Accepted: 7 April 2023 / Published online: 26 April 2023

Abstract
In this study, we combined the geochemical characteristics based on Rock-Eval pyrolysis and gas chromatography – mass spectrometry (GC–MS) results with the facies analysis. These surveys were conducted within grey to black claystones/mudstones intervals of the Podil'tsi and Kokhanivka formations, related to the Pliensbachian and Toarcian–Bathonian ages, respectively. The geochemical results revealed that the Podil'tsi Formation contains mixed marine/terrigenous, early-mature to mature organic matter. The deposition of this formation took place in dysoxic redox conditions of a sulphate-poor marine palaeoenvironment, with oxygen scarcity within the photic zone, as documented by green- and brown-pigmented Chlorobiaceae. Oleanane is present within the samples from the Podil'tsi Formation, which is uncommon within Lower Jurassic sedimentary rocks. The Kokhanivka Formation contains mostly early-mature, terrestrial organic matter, deposited in suboxic conditions of a sulphate-poor, fluvial–deltaic palaeoenvironment. The absence of aliphatic diterpenoids within the Middle Jurassic strata points to the low significance of conifers in the sediment supply area at this time. All of the Podil'tsi and most of the Kokhanivka formations are characterised by poor hydrocarbon potential. Only the middle part of the Kokhanivka Formation, built by brown, organic-rich claystones, shows fair-to-good hydrocarbon potential. Based on our results, a chemostratigraphic correlation of the Toarcian–Bathonian strata from the Carpathian Foredeep with the same strata from the neighbouring Polish Basin was performed. The juxtaposition of the geochemical and facies results suggests that the interval of brown organic-rich claystones, from the middle part of the Kokhanivka Formation can be related to the Middle–Upper Aalenian Age.

Keywords Jurassic · Oleanane · Chemostratigraphy · Ukraine · Rock Eval · GC–MS

Introduction

Chemostratigraphy surveys focuses on the investigation of the inorganic/organic geochemistry parameter variations across the sedimentary sequences. This technique can be based, for example, on the molecular composition of the rock to reveal stratigraphic relationships (e.g. Slatt et al. 2021; Silva Souza et al. 2022). A chemostratigraphy can be made such as by advanced and complex analysis comparing the biomarker distribution. Biomarkers are molecular fossils derived from biochemical compounds, which are the remnants of ancient organisms. Due to the possibility of investigating the diagenetic evolution pathways of chemical compounds, the biomarkers can be used to describe organic matter's origin and maturity, as well as the palaeoenvironmental conditions (e.g. Peters et al. 2005).

Biomarkers were used extensively to describe the organic matter's origin and palaeoenvironmental conditions within the Lower and Middle Jurassic strata from the epicontinental seas located at the Central European Basin System area (Fig. 1c) (e.g. Schwark and Frimmel 2004; Song et al. 2017; Ruebsam et al. 2020; Zakrzewski et al. 2020, 2022a, b). Surveys conducted predominately in the southeast direction, in the Mesozoic basement of the Carpathian Foredeep wherein

✉ Adam Zakrzewski
zakrzewski@agh.edu.pl

[1] Faculty of Geology, Geophysics and Environmental Protection, AGH-University of Science and Technology, Al. A. Mickiewicza 30, 30–059 Kraków, Poland

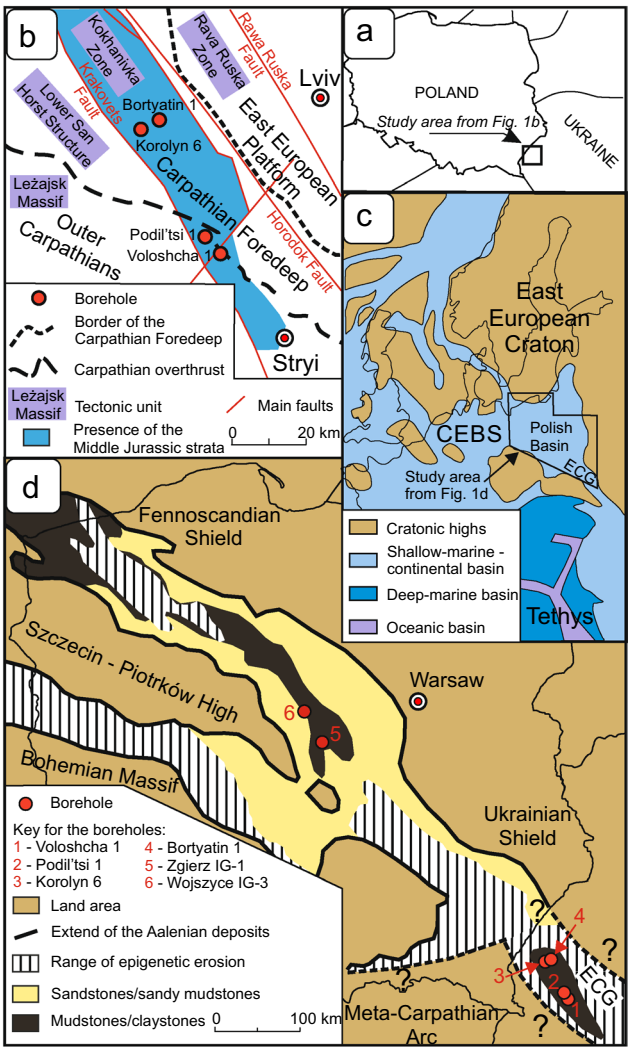

Fig. 1 **a** Study area at the nowadays' state borders' background. **b** Localisation map of the studied boreholes with the simplified borders of the main geological and tectonic units (both modified after Krajewski et al. 2011). **c** Middle Jurassic palaeogeographical map illustrating the localisation of the East Carpathian Gate (after Ziegler 1990) and **d** Middle Aalenian – Lower Bajocian palaeogeographical map with localisation of the boreholes from the Polish Basin and East Carpathian Gate areas, used for the correlation of the Rock-Eval pyrolysis results between these two areas (map modified after Feldman-Olszewska 1997; Marek and Pajchlowa 1997). **Key**: *CEBS* Central European Basin System, *ECG* East Carpathian Gate

the Middle Jurassic epoch the East Carpathian Gate (ECG) was located (Fig. 1c), were focused mostly on the hydrocarbon potential of the Jurassic horizons, rather than presenting a detailed description of the palaeoenvironmental conditions and organic matter origin (e.g. Kotarba et al. 2011a; Kosakowski, et al. 2012; Rauball et al. 2020). Moreover, some previous works (e.g. Kotarba et al. 2011a; Kosakowski, et al. 2012) were based on obsolete stratigraphy, which was critically examined by biostratigraphic data (e.g. Zhabina et al. 2017). It should be noted that Zakrzewski and Kosakowski's (2021) work was based on stratigraphical identification from Kosakowski et al. (2012), where all the samples from the Voloshcha 1 borehole were classified as the Upper Jurassic strata. In this paper, based on facies analyses and the literature (e.g. Zhabina et al. 2017), we changed their identification to the Lower–Middle Jurassic strata (Fig. 2).

For these reasons, we combined sedimentological and geochemical data to describe Jurassic formations recognised within four boreholes: Bortyatin 1, Korolyn 6, Podil'tsi 1, and Voloshcha 1 (Fig. 1).

In the investigated boreholes, the sedimentological analysis allowed us to distinguish (i) Lower–Middle Jurassic and (ii) Middle Jurassic–Lower Cretaceous sedimentary complexes separated by an erosive surface between Bathonian and Callovian sediments. Lower–Middle Jurassic sedimentary succession is dominated by siliciclastic facies types ([FTs] 1–6), while the Middle Jurassic–Lower Cretaceous sedimentary complex is dominated by carbonate facies (Dulub et al. 2003; Krajewski et al. 2011, 2020). For this reason, FTs have been allocated to each sedimentary complex separately. This paper dealt with the Podil'tsi and Kokhanivka formations (Fms.), referring to the Pliensbachian and Toarcian–Bathonian ages, respectively (Fig. 2) (e.g. Zhabina et al. 2017).

This work aimed to present the detailed palaeoenvironmental conditions and organic matter origin from both the Podil'tsi and Kokhanivka Fms. Based on information from geochemical (Rock-Eval pyrolysis and gas chromatography – mass spectrometry [GC–MS]) and sedimentological surveys, we presented the main differences between these formations. A combination of geochemical and sedimentological results pave the way for correlation between the analysed boreholes. The juxtaposition of geochemical and sedimentological data from this study with the geochemical data published for the Lower and Middle Jurassic strata from the Polish Basin (PB) will allow a chemostratigraphic correlation between the ECG and PB. This will show the potential to use Rock-Eval pyrolysis in chemostratigraphic correlation.

The second scientific goal is to show the detailed hydrocarbon potential across the Podil'tsi and Kokhanivka Fms. within the analysed boreholes. This is needed as Kosakowski et al.'s (2012) study described the data from these boreholes based on obsolete stratigraphy, and did not present detailed Rock-Eval pyrolysis results for the boreholes surveyed in this study.

Geological settings

The Mesozoic sediments from the western Ukrainian part of the Carpathian Foredeep basement were recognised in numerous boreholes (Fig. 1) (e.g. Dulub et al. 2003; Gutowski et al. 2005; Karpenchuk et al. 2006; Zhabina and

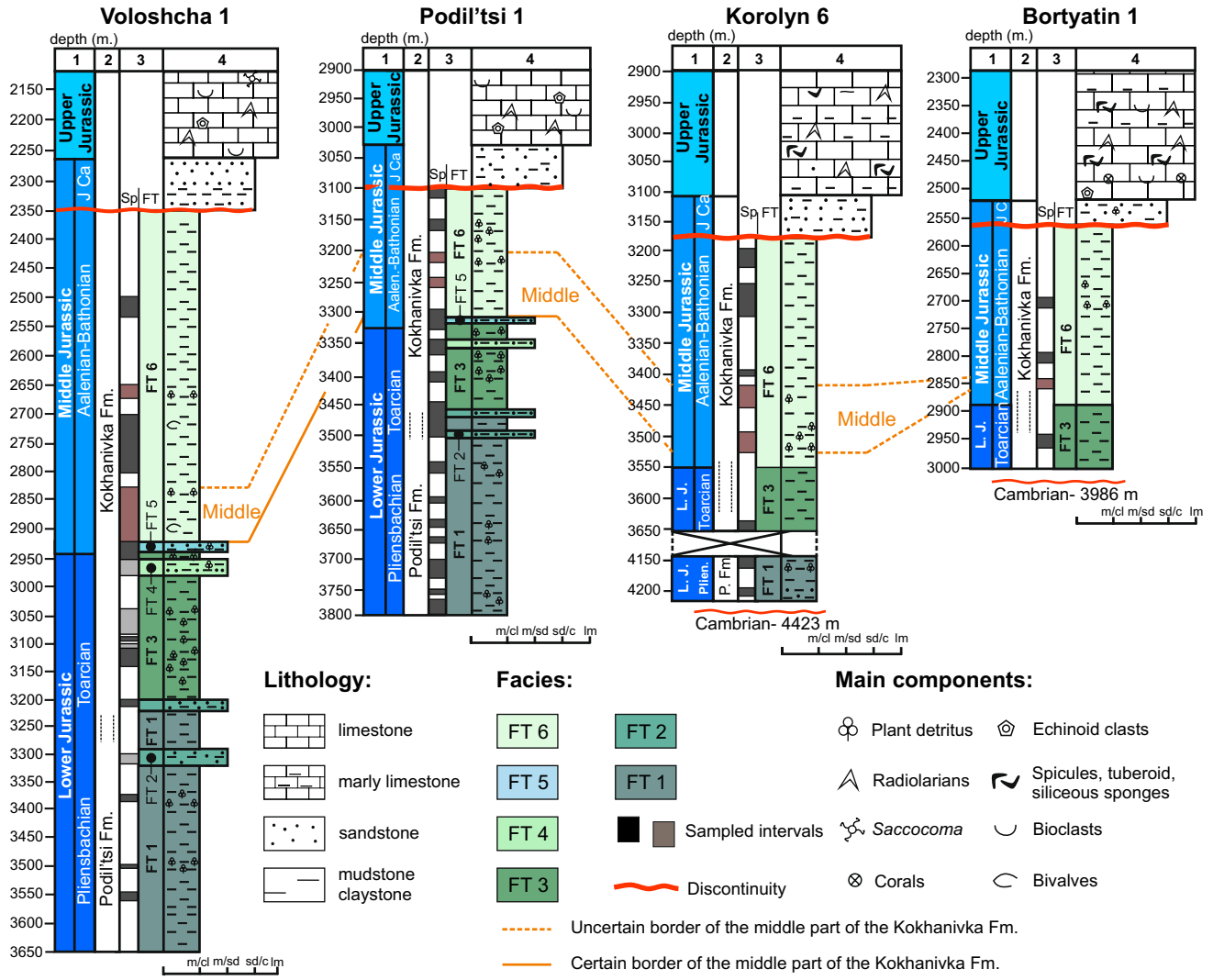

Fig. 2 Lithostratigraphical logs of the Lower–Middle Jurassic sedimentary succession recorded in the boreholes cored in the Ukrainian part of the Carpathian Foredeep basement. (1) stratigraphy; (2) lithostratigraphical formations (modified after Zhabina et al. 2017); (3) cored intervals, the colour of the core and facies types (FT 1–6); (4) lithology: (m) – mudstone, (cl) – claystone, (sd) – sandstone, (lm) – limestone

Anikeyeva 2007; Krajewski et al. 2011, 2020). The study area is located along the southwest margin of the East European Platform between the Horodok Fault (Buła and Habryn 2011) in the northeast, and the Krakovets Fault in the southwest known as the Bilche–Volytsia Zone (e.g. Karpenchuk et al. 2006; Krajewski et al. 2011; Zhabina et al. 2017). The block character of the Palaeozoic basement structure and the tectonic activity of the main transcontinental dislocations have substantially influenced the development and thickness of Mesozoic deposits on the Carpathian Foredeep basement (e.g. Karpenchuk et al. 2006; Buła and Habryn 2011; Krajewski et al. 2011). The Mesozoic sedimentary succession overlies eroded Palaeozoic, mainly the Cambrian basement (Buła and Habryn 2011), and is primarily overlapped by the Neogene formations (e.g. Karpenchuk et al. 2006; Kurovets et al. 2011). In the study area, the Mesozoic sediments are represented by three main sedimentary complexes: (i) the clastic Lower–Middle Jurassic (Hettangian–Bathonian), (ii) the mainly carbonate Middle Jurassic (Callovian)–Lower Cretaceous (up to Barremian), and (iii) the mixed carbonate–siliciclastic Upper Cretaceous (Cenomanian–Turonian) (e.g. Dulub et al. 2003; Świdrowska et al. 2008; Kotarba et al. 2011b; Krajewski et al. 2011, 2020; Zhabina et al. 2017). The two youngest sedimentary complexes were not investigated in this paper.

The Lower–Middle Jurassic sedimentary succession was divided into five lithostratigraphic formations: (i) the Hettangian Komarno Fm., (ii) the Sinemurian Bortyatin Fm., (iii) the Pliensbachian Podil'tsi Fm., (iv) the Toarcian Medenychi Fm., and (v) the Toarcian–Bathonian Kokhanivka Fm. (e.g.

Dulub et al. 2003; Zhabina et al. 2017) dated biostratigraphically based on palynological studies of spores and pollen, but rarely on the foraminifera and molluscs' characteristics (e.g. Gareckij 1985; Dulub et al. 2003; Zhabina et al. 2017). Within the mentioned formations and between them there are erosional surfaces related to the evolution of sedimentary basin, especially tectonic phases and transgressive–regressive cycles (e.g. Dulub et al. 2003; Karpenchuk et al. 2006; Zhabina et al. 2017).

Materials and methods

Samples

One hundred and twenty-five core samples were collected for facies examination. All samples are represented by grey, brown, or black claystones/mudstones (Fig. 2). For the geochemical surveys, 60 core samples were sampled. All these samples were analysed by Rock-Eval II pyrolysis. After that, representative samples from each formation and borehole were selected and surveyed by GC–MS. Finally, 15 samples were analysed by GC–MS.

Facies analysis

The basic sedimentological research method was the analysis of drill cores taken from wells drilled in the Carpathian Foredeep basement. The biostratigraphical data has been adopted from previous publications (Dulub et al. 2003; Zhabina and Anikeyeva 2007; Olszewska et al. 2012; Zhabina et al. 2017). The described FTs were correlated with the existing lithostratigraphic formations (Fig. 2). These enabled lithostratigraphic correlations of the new presented lithological logs and described facies' succession of the study area.

Rock-Eval pyrolysis

In this paper, we used the Rock-Eval pyrolysis results that emerged from Kosakowski et al. (2012) work. Rock-Eval pyrolysis analyses were performed to obtain the basic geochemical parameters such as TOC, $S_1 + S_2$, and T_{max} temperature. These analyses were performed using a Rock-Eval II instrument equipped with a TOC module, based on the procedure described by Espitalié et al. (1977).

The pyrolysis of organic matter was performed over a temperature range of 300–600 °C with a temperature increase of 25 °C/min. The following parameters were measured: S_1 (mg HC/g rock) – free hydrocarbons; S_2 (mg HC/g rock) – hydrocarbons cracked during pyrolysis; S_3 (mg CO_2/g rock) – CO_2 originated during pyrolysis; S_4 (mg C/g rock) – residual carbon; and T_{max} (°C) – maximum temperature of peak S_2. These parameters were used to determine the total organic carbon – TOC (wt. %) = $[0.082(S_1 + S_2) + S_4]/10$, S_1/TOC ratio, production index – PI = $[S_1/(S_1 + S_2)]$, hydrogen index – HI (mg HC/g TOC) = $(100 \times S_2/\text{TOC})$, and oxygen index – OI (mg CO_2/g TOC) = $(100 \times S_3/\text{TOC})$.

The Rock-Eval pyrolysis measurements were calibrated using the IFP160000 standard. In some cases, parts of the Rock-Eval pyrolysis results were denoted as unreliable (Supplementary Appendix 1). The HI values were not interpreted for TOC ≤ 0.2 wt%, and the T_{max} values were rejected in the situation when $S_2 \leq 0.3$ mg HC/g and/or the flat pyrogram made it impossible to properly identify the T_{max} value (Peters 1986).

Gas chromatography – mass spectrometry (GC–MS)

Samples were milled to a fraction of < 0.2 mm. After that, samples were extracted with dichloromethane:methanol (93:7 v/v) in a Soxleth™ apparatus. The asphaltene fraction was precipitated with *n*-hexane. The remaining maltenes were then separated into compositional fractions of aliphatic hydrocarbons, aromatic hydrocarbons, and resins by means of column chromatography, using an alumina:silica gel (2:1 v/v) column (0.8 × 25 cm). The fractions were eluted with *n*-hexane, toluene, and toluene:methanol (1:1 v/v), respectively. Each fraction was evaporated to dryness by leaving the glass crystalliser with the fraction on the fume cupboard for 12 h at room temperature about 20 °C. This laboratory protocol excluded the possibility of losing the light molecular weight compounds (Ahmed and George 2004).

The aliphatic fraction isolated from the bitumens was diluted in isooctane and analysed with the GC–MS for biomarker determination. The analysis was carried out with the Agilent 7890A gas chromatograph equipped with the Agilent 7683B automatic sampler, an *on-column* injection chamber, and a fused silica capillary column (60 m × 0.25 mm i.d.) coated with 95% methyl/5% phenylsilicone phase (DB-5MS, 0.25 µm film thickness). Helium was used as a carrier gas. The GC oven was programmed with the next steps: 99 °C held for 1 min, then increased to 310 °C at the rate of 2 °C/min, and held at 310 °C for 45 min. The run time of the analysis was nearly 150 min. The gas chromatograph was coupled with the 5975C mass selective detector (MSD). The MS operated at an ion source temperature of 230 °C, ionisation energy of 70 eV, and a cycle time of 1 s in the mass range from 45 to 500 Da. The analysis of the aromatic hydrocarbon fraction was carried out using the same equipment as for the saturated hydrocarbon fraction. The GC oven was programmed from 40 to 300 °C at the rate of 3 °C min^{-1}. The MS operated with a cycle time of 1 s in the mass range from 45 to 550 Da.

Identification of individual compounds was made possible by identifying peaks on the chromatogram containing the desired fragmentation ions and characterised by the expected

retention time. The concentrations of the compounds used in all formulas were calculated based on the base peak area at the characteristic mass fragmentograms (Supplementary Appendix 2). For example, for cadalene the peak area from m/z 183 mass fragmentogram was used in all formulas. Abbreviations of the chemical compounds were enlisted in Supplementary Appendix 2. The formula used to calculate of biomarker ratio mentioned in the text is always placed in the footnote of the table containing this formula.

Results

Facies

The oldest sedimentary successions presented in this work represent the Podil'tsi Fm. and are formed by rhythmic interbedding dark grey mudstone/claystone facies (FT 1; Fig. 2). The upper part of the formation also includes grey cross-bedded mudstone/sandstone facies (FT 2) with thin interlayers of limestones and thin streaks or nest-like anhydrite. Along intervals, plant detritus was commonly observed.

Higher in the sedimentary succession is the Kokhanivka Fm.; however, in the studied boreholes, the border with the Podil'tsi Fm. is unclear. The lower part of the Kokhanivka Fm. related to the Toarcian Age is dominated by dark grey and grey mudstone/claystone facies (FT 3), and cross-bedded fine- and medium-grained grey mudstone/sandstone facies (FT 4) with lenses and interlayers of coal and sandstones with streaks of clays, mudstones and thin layers of beige-grey limestones. The facies contain coalified fitodetrit and imprints of plants.

The Middle Jurassic strata are represented mostly by the middle and upper parts of the Kokhanivka Fm. In the lower part of the Middle Jurassic, there are grey mudstone/sandstone facies (FT 5) with gravel intercalations. The Middle Jurassic part of the Kokhanivka Fm. is mainly created by marine dark grey, brown, and almost black claystone/mudstone facies (FT 6) with molluscs, interbedded with micaceous mudstone facies. Thin intercalations of dark grey bioclastic limestone facies with bivalves were also observed. Plant debris is common throughout this formation.

In the analysed boreholes, we concluded that the Medenychi Fm. is absent, and as above the Podil'tsi Fm we observed claystones/mudstones instead of sandstones (Fig. 2). In this case, the Kokhanivka Fm. possesses a relatively wide stratigraphical range (Toarcian–Bathonian; Zhabina et al. 2017). For this reason, we divided the Kokhanivka Fm. into three parts: (i) a lower part, related to the Toarcian–Lower Aalenian (an equivalent of the Medenychi Fm.); (ii) a middle part, related to the Middle–Upper Aalenian; and (iii) an upper part, related to the Bajocian–Bathonian Age. This division can be supported by the lithology and similarities to Middle Jurassic deposition in the PB, which was temporarily linked with the ECG (e.g. Feldman-Olszewska 1997). We propose that the organic-rich middle part of the Kokhanivka Fm. corresponds to the Middle–Upper Aalenian organic-rich claystones and mudstones from the PB (e.g. Zakrzewski et al. 2022a).

Rock-Eval pyrolysis

The results of the Rock-Eval pyrolysis were gathered in Table 1 and Supplementary Appendix 1. The results from the Podil'tsi and Kokhanivka Fms. were presented separately. The TOC results vary from 0.08 to 1.92 and from 0.07 to 12.12 for the Podil'tsi and Kokhanivka Fms., respectively. Some of the T_{max}, $S_1 + S_2$, and HI values were recognised as unreliable (Supplementary Appendix 1). Among the remaining results, the T_{max} results vary from 427 °C to 447 °C within the Kokhanivka Fm., and from 439 °C to 449 °C within the Podil'tsi Fm. The $S_1 + S_2$ results fall in the range from 0.05 to 1.71 and from 0.23 to 13.96 for the Podil'tsi and Kokhanivka Fms., respectively. Higher HI results from 33 to 164 were observed within the Kokhanivka Fm., while the Podil'tsi Fm. is characterised by a few HI values that vary from 0 to 88 (Table 1).

Biomarkers

Organic matter's maturity

As the maturity of the analysed strata was described in previous papers (e.g. Kosakowski et al. 2012; Rauball et al. 2020), we calculated only a few basal maturity indicators to show

Table 1 Selected results of Rock-Eval pyrolysis

Fm	Q	TOC [wt. %]				T_{max} [°C]				$S_1 + S_2$ [mg HC/ g rock]				HI [mg HC/ g TOC]			
		Avg	Min	Max	Med	Avg	Min	Max	Med	Avg	Min	Max	Med	Avg	Min	Max	Med
Koh	51	3.30	0.07	12.12	1.92	436	427	447	435	3.64	0.23	13.96	1.97	87	33	164	83
Pod	9	0.50	0.08	1.92	0.15	446	439	449	449	0.65	0.05	1.71	0.66	44	0	88	50

Key: *Fm.* formation, *Koh* Kokhanivka, *Pod* Podil'tsi, *Q* quantity of Rock-Eval analyses, *Avg* average value, *Min* minimum value, *Max* maximum value, *Med* median value

the possible maturity influence on biomarker distribution. Among them were $C_{29}\beta\beta/(\alpha\alpha+\beta\beta)$, $C_{29}20S/(S+R)$, and $C_{31}S/(S+R)$. The results of two indicators based on stigmastanes, that is, $C_{29}\beta\beta/(\alpha\alpha+\beta\beta)$ and $C_{29}20S/(S+R)$, vary from 0.25 to 0.56 and from 0.10 to 0.53, respectively. The $C_{31}S/(S+R)$ results fall in the range of 0.44–0.59 (Table 2).

Origin of organic matter

A set of various biomarker compounds and indicators presented in Tables 3 and 4 was used to describe the organic matter's origin within the analysed strata.

Analysis of the fragmentation ion *m/z* 71 revealed the presence of *n*-alkanes from the C_{15} to C_{35} homologues. Most of the samples are characterised by the unimodal distribution of *n*-alkanes, and the dominant homologues vary in dependency on the formation (Table 3). Short-chain *n*-alkanes have the highest abundance within the Lower Jurassic Podil'tsi Fm. (Table 3; Fig. 3c–d). Mid-chain compounds play a dominant role within the Middle Jurassic part of the Kokhanivka Fm. (Table 3; Fig. 3b). Long-chain *n*-alkanes play a crucial role in most of the samples from the lowermost (Lower Jurassic) part of the Kokhanivka Fm. (Table 3; Fig. 3a).

Based on the *n*-alkane distribution several indicators were calculated. Among them were the long-to-short hydrocarbon ratio (LTS_{HC}), and the proxy aquatic ratio (P_{aq}). The LTS_{HC} results vary from 0.20 to 1.39 within the Podil'tsi Fm., and from 0.40 to 19.6 within the Kokhanivka Fm. The P_{aq} results vary from 0.41 to 0.65 within the Podil'tsi Fm. and from 0.61 to 0.96 within the Kokhanivka Fm. (Table 3).

7- and 8-monomethyl alkanes (MMA) were present in the Kokhanivka Fm. from the Korolyn-6 and Bortyatin 1 boreholes, and in all analysed samples from the Podil'tsi Fm. (Table 3).

Two acyclic isoprenoids, pristane (Pr) and phytane (Ph), were also marked at *m/z* 71 chromatograms. Due to a lack of Pr and/or Ph, these ratios were not calculated within four samples from the Kokhanivka Fm. The Pr/C_{17} and Ph/C_{18} results vary from 0.33 to 19.7 and from 0.29 to 1.96, respectively (Table 3).

Sterane distribution was marked at *m/z* 217 mass ion chromatograms, which led to the calculation of the regular sterane distribution (Table 3). The distribution of regular steranes revealed that C_{29} regular steranes have a dominant role within the samples from the Kokhanivka Fm. (Table 3). In most of the samples referred to the Podil'tsi Fm., regular sterane distribution is also characterised by the highest abundance of C_{29} sterane, but the domination is not as high as that within the Kokhanivka Fm. (Table 3). Based on the regular steranes versus 17α hopanes content, the sterane/hopane (S/H) ratio was calculated (Peters et al. 2005), with all the obtained S/H results below 1 (Table 3).

The analysed samples from the Podil'tsi Fm. contain aromatic carotenoids as well as aliphatic diterpanes and oleanane (Tables 3, 4). Within the Kokhanivka Fm., aromatic carotenoids are sparse. Aliphatic diterpanes within the Kokhanivka Fm. were observed only within the lower part of the formation (Tables 3, 4). Oleanane was marked only within samples from the Podil'tsi Fm. The oleanane index results vary from 1.46 to 6.45 (Table 3).

Plant-derived aromatic biomarkers were common in both the Podil'tsi and Kokhanivka Fms. (Table 4). Amongst them were retene (Ret), cadalene (Cad), and 6-isopropyl,1-isohexyl,2-methylnapthaplene (*ip-i*HMN), which were used

Table 2 Biomarker indicators linked with organic matter maturity

Borehole	Depth	Str	Form	$C_{29}\ \beta\beta/(\alpha\alpha+\beta\beta)$	$C_{29}\ S/(S+R)$	$C_{31}\ S/(S+R)$	Per
Bortyatin 1	2846	J_2	Koh	0.34	0.27	0.56	+
Korolyn 6	3421	J_2	Koh	0.31	0.34	0.58	+
Korolyn 6	3517	J_2	Koh	0.39	0.53	0.58	+
Podiltsi 1	3214	J_2	Koh	0.25	0.34	0.57	+
Voloshcha 1	2659	J_2	Koh	0.34	0.10	0.50	+
Voloshcha 1	2870	J_2	Koh	0.33	0.21	0.53	+
Voloshcha 1	2903	J_2	Koh	0.37	0.15	0.54	+
Korolyn 6	3642	J_1	Koh	0.44	0.59	0.58	
Podiltsi 1	3316	J_1	Koh	0.38	0.38	0.59	+
Voloshcha 1	2952	J_1	Koh	0.31	0.28	0.55	+
Voloshcha 1	3126	J_1	Koh	0.31	0.38	0.56	+
Korolyn 6	4157	J_1	Pod	0.53	0.44	0.54	
Podiltsi 1	3475	J_1	Pod	0.45	0.45	0.58	+
Voloshcha 1	3370	J_1	Pod	0.46	0.38	0.57	+
Voloshcha 1	3547	J_1	Pod	0.49	0.38	0.57	+

Key: *Str* stratigraphy, J_2 Middle Jurassic, J_1 Lower Jurassic, *Form.* Formation, *Koh* Kokhanivka, *Pod* Podil'tsi, *Per* perylene, "+" present

Table 3 Biomarker indicators (aliphatic fraction) linked with organic matter's origin

Borehole	Depth	FT	Str	Fm	High n-Cx	LTS_{HC}	Pr/C_{17}	Ph/C_{18}	P_{aq}	Regular steranes [%]			S/H	MMA	Oleanane index	Diterpanes				
										C_{27}	C_{28}	C_{29}				NIP	Fi	IP	Abt	16a-Phyl
Bortyatin 1	2846	FT6	J_2	Koh	25	1.60	4.21	0.70	0.70	23	22	55	0.05	+						
Korolyn 6	3421	FT6	J_2	Koh	23	2.02	n.c	0.39	0.79	23	17	60	0.07	+						
Korolyn 6	3517	FT6	J_2	Koh	21	0.73	1.19	0.29	0.96	35	17	48	0.03	+						
Podiltsi 1	3214	FT6	J_2	Koh	23	6.85	n.c	n.c	0.84	22	17	61	0.05							
Voloshcha 1	2659	FT6	J_2	Koh	25	19.6	n.c	n.c	0.66	27	18	55	0.15							
Voloshcha 1	2870	FT6	J_2	Koh	23	2.02	7.88	0.82	0.81	24	10	67	0.04							
Voloshcha 1	2903	FT6	J_2	Koh	23	10.6	n.c	1.23	0.74	15	19	66	0.04							
Korolyn 6	3642	FT3	J_1	Koh	15	0.40	0.63	0.19	0.76	27	22	51	0.08	+			+	+	+	
Podiltsi 1	3316	FT3	J_1	Koh	27	4.61	19.67	1.40	0.63	7	14	79	0.11							tr
Voloshcha 1	2952	FT4	J_1	Koh	25	2.25	7.56	1.10	0.64	13	19	67	0.05			tr				
Voloshcha 1	3126	FT3	J_1	Koh	27	1.80	2.14	0.46	0.61	25	12	63	0.19			tr			tr	
Korolyn 6	4157	FT1	J_1	Pod	20	0.73	0.33	0.34	0.65	19	37	44	0.28	+	1.46				+	
Podiltsi 1	3475	FT1	J_1	Pod	20	1.39	0.88	0.58	0.56	17	33	49	0.12	+	1.48				+	+
Voloshcha 1	3370	FT1	J_1	Pod	18	0.20	0.86	0.49	0.53	20	37	42	0.31	+	6.21				+	+
Voloshcha 1	3547	FT1	J_1	Pod	18	0.49	0.97	0.57	0.41	17	42	41	0.34	+	6.45				+	+

Key: *Str* stratigraphy, J_2 Middle Jurassic, J_1 Lower Jurassic, *Fm.* formation, Koh Kokhanivka, Pod Podil'tsi, n-Cx n-alkane, LTS_{HC} (n-C_{27}+n-C_{28}+n-C_{29})/(n-C_{17}+n-C_{18}+n-C_{19}) (Kosakowski et al. 2012), P_{aq} (n-C_{23}+n-C_{25})/(n-C_{23}+n-C_{25}+n-C_{29}+n-C_{31}) (Ficken et al. 2000), *S/H* sterane/hopane, *MMA* monomethyl alkanes, oleanane index=(oleanane/C_{30}H)*100 (Peters et al. 2005), *NIP* norisopimarane, *Fi* fichtellite, *IP* isopimarane, *Abt* abietane, 16a-Phyl 16a-phyllocladane, "+" present, *tr* traces, *n.c.* not calculated. All depth values in metres

Table 4 Biomarker indicators (aromatic fraction) linked with organic matter origin

Borehole	Depth	Str	Fm	Ar carot		BeP/(BeP + BaP)	Plant-derived aromatic biomarkers							PF			(*ip*-*i*HMN + Ret)/Ret	(Sim + MeRet + Ret)/Ret
				IRen	Ren		Cad	Ret	DiT	Sim	*ip*-*i*HMN	DAME	MeRet	Cad	Ret	*ip*-*i*HMN		
Bortyatin 1	2846	J_2	Koh			0.52	+	+	+	+	+		+	2	89	9	1.10	1.07
Korolyn 6	3421	J_2	Koh			0.73	+	+			+	+	+	0	97	3	1.03	1.08
Korolyn 6	3517	J_2	Koh			0.79	+	+			+		+	1	94	5	1.06	1.27
Podiltsi 1	3214	J_2	Koh			0.54	+	+	+	+	+	+	+	0	91	9	1.10	1.09
Voloshcha 1	2659	J_2	Koh			0.45		+		+	+	+	+	0	95	5	1.06	1.11
Voloshcha 1	2870	J_2	Koh			0.45	+	+	+	+	+		+	2	85	13	1.15	1.14
Voloshcha 1	2903	J_2	Koh			0.47	+	+	+	+	+	+	+	1	85	14	1.17	1.09
Korolyn 6	3642	J_1	Koh		+	0.85	+	+			+	+	+	21	79	0	1.00	1.27
Podiltsi 1	3316	J_1	Koh			0.57	+	+	+	+	+		+	10	54	36	1.66	1.38
Voloshcha 1	2952	J_1	Koh			0.37	+	+	+	+	+		+	12	39	49	2.26	1.82
Voloshcha 1	3126	J_1	Koh			0.61	+	+	+	+	+	+	+	4	78	18	1.23	1.22
Korolyn 6	4157	J_1	Pod	+	+	0.83	+	+			+	+	+	0	98	2	1.10	1.25
Podiltsi 1	3475	J_1	Pod	tr	tr	0.62	+	+			+	+	+	0	91	9	1.02	1.23
Voloshcha 1	3370	J_1	Pod	+	+	0.82	+	+			+	+	+	1	84	15	1.18	1.09
Voloshcha 1	3547	J_1	Pod	tr	tr	0.88		+			+	+	+	0	86	14	1.16	1.07

Key: *Str* stratigraphy, J_2 Middle Jurassic, J_1 Lower Jurassic, *Fm*. formation, *Koh* Kokhanivka, *Pod* Podil'tsi, *Ar carot* aromatic carotenoids, *IRen* isorenieratane, *Ren* renieratane, *BeP* benzo[e] pyrene, *BaP* benzo[a]pyrene, *Cad* cadalene, *Ret* retene, *DiT* diaromatic totarane, *Sim* simonellite, *ip-iHMN*—6-isopropyl,1-isohexyl,2-methylnaphthalene, *DAME* dehydrabietic acid methyl ester, *MeRet* 2-methylretene, *PF* plant fingerprint (Cesar and Grice 2019), "+" present, *tr* traces, All depth values in metres

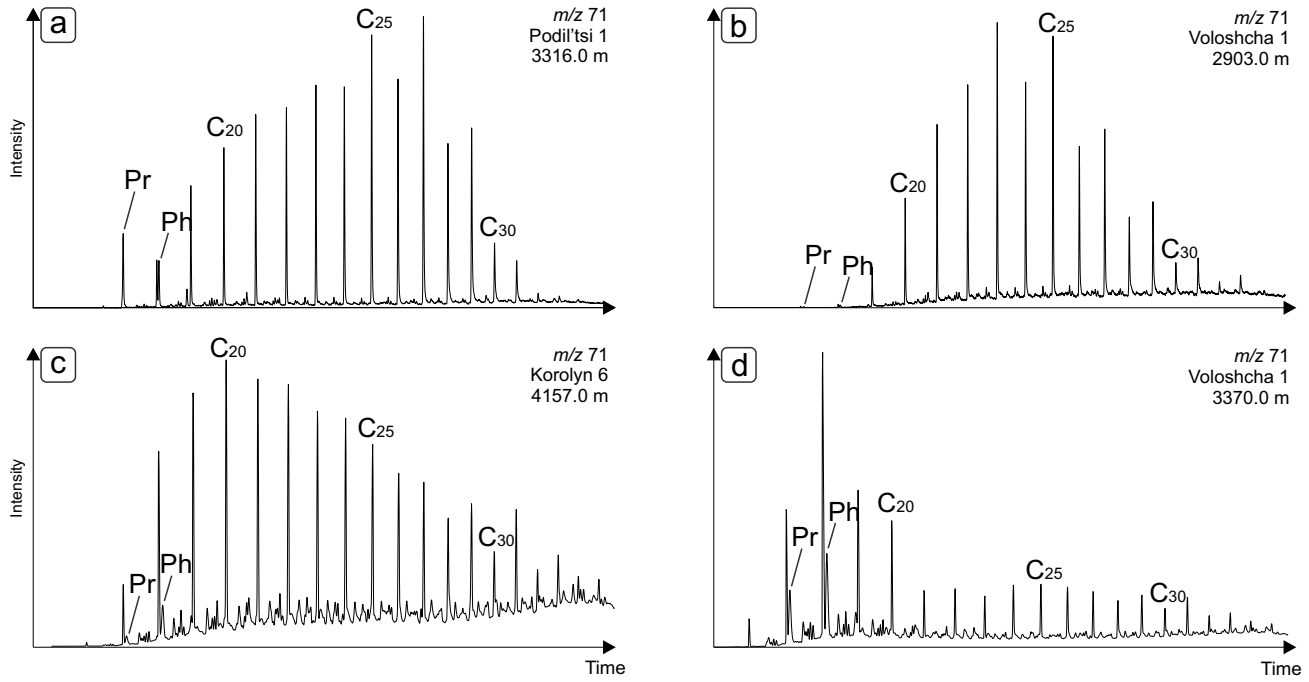

Fig. 3 Mass chromatograms of *m/z* 71 with *n*-alkane distribution for **a–b** Kokhanivka Fm. and **c–d** Podil'tsi Fm

to show the "plant fingerprint" (PF) (Table 4) (Cesar and Grice 2019). Also, simonellite (Sim), dehydroabietic acid methyl ester (DAME), 2-methylretene (MeRet), and diaromatic totarane (DiT) were recognised.

Palaeoenvironmental conditions

Palaeoenvironmental conditions including redox conditions, palaeosalinity, palaeo-wildfire activity, and palaeogeography are described by the biomarker indicators presented in Table 5.

The Pr/Ph results vary from 0.27 to 0.68 and from 0.53 to 3.13 within the Podil'tsi and Kokhanivka Fms., respectively. To support the obtained Pr/Ph results, the homohopanes' distribution was calculated. In most of the samples, tetra- and pentahomohopanes are present and represent 4–22% of the total homohopanes content (Table 5). Pentahomohopanes were absent only in the four samples from the middle and upper part of the Kokhanivka Fm. from the Podil'tsi 1 and Voloshcha 1 boreholes, which led to the absence of $C_{35}S/C_{34}S$ results (Table 5).

For the Podil'tsi Fm., the results of the $C_{29}H/C_{30}H$ and $C_{35}S/C_{34}S$ ratios vary from 0.58 to 1.02 and from 0.66 to 0.98, respectively. Within the analysed Kokhanivka Fm., $C_{29}H/C_{30}H$ and $C_{35}S/C_{34}S$ vary from 0.61 to 1.26 and from 0.19 to 0.63, respectively (Table 5).

The dibenzotiophene/phenanthrene (DBT/Phen) ratio results are low in both analysed formations and do not exceed 0.10 (Table 5). Simultaneously, the gammacerane index (GI) ratio also indicates low values that do not reach 0.10 (Table 5).

Furthermore, the samples contain a series of polycyclic aromatic hydrocarbons (PAHs). Amongst them are fluoranthene (Fl) and pyrene (Py) (*m/z* 202), benzo[a]anthracene (BaA), triphenylene and chrysene (Chr) (*m/z* 228), benzofluoranthenes, benzo[e]pyrene (BeP), benzo[a]pyrene (BaP), perylene (Per) (*m/z* 252), indeno(1,2,3,cd-)pyrene, benzo[*ghi*]perylene (BgP) (*m/z* 276), and coronene (*m/z* 300). Based on the *m/z* 202 and *m/z* 228 mass fragmentograms, the Fl/(Fl + Py) and BaA/(BaA + Chr) ratios were calculated. Their values within the Podil'tsi Fm. vary from 0.36 to 0.53 and from 0.03 to 0.18, respectively. Within the Kokhanivka Fm., these ratios vary from 0.40 to 0.62 and from 0.13 to 0.57, respectively.

The abundance of PAHs mentioned above was also used to calculate a few indicators: BeP/(BeP + BaP) (Table 4), the pyrolytic input ratio (PIR), low molecular weight PAHs/Total PAHs (LMW/Total), and BgP/(Per + BgP) (Table 5). BeP/(BeP + BaP) vary from 0.62 to 0.88 within the Podil'tsi Fm., and from 0.37 to 0.79 within the Kokhanivka Fm. The PIR and LMW/Total results within the Podil'tsi Fm. vary from 22.2 to 91.3 and from 0.15 to 0.32, respectively (Table 5). The Kokhanivka Fm. samples are characterised by PIR and LMW/Total in ranges from 3.30 to 42.8 and from 0.18 to 0.51, respectively. The BgP/(Per + BgP) results vary from 0.73 to 1.00 and from 0.32 to 0.91 for the Podil'tsi and Kokhanivka Fms., respectively (Table 5).

Table 5 Biomarker indicators linked with palaeoenvironmental conditions

Borehole	Depth	Str	Form	Pr/Ph	DBT/Phen	GI	$C_{29}H/C_{30}H$	$C_{35}S/C_{34}S$	Homohopane distribution [%]					Fl/(Fl + Py)	BaA/(BaA + Chr)	PIR	LMW/Total	BgP/(Per + BgP)
									C_{31}	C_{32}	C_{33}	C_{34}	C_{35}					
Bortyatin 1*	2846	J_2	Koh	1.12	0.03	n.c	0.76	0.30	58	22	9	8	2	0.54	0.51	22.7	0.36	0.45
Korolyn 6*	3421	J_2	Koh	n.c	0.05	0.04	0.79	0.41	54	23	12	8	3	0.50	0.25	42.8	0.30	0.82
Korolyn 6*	3517	J_2	Koh	0.53	0.03	0.02	0.77	0.19	53	25	13	7	2	0.49	0.27	22.8	0.51	0.83
Podiltsi 1*	3214	J_2	Koh	n.c	0.03	0.01	0.90	0.00	60	25	10	6	0	0.50	0.47	13.4	0.24	0.48
Voloshcha 1*	2659	J_2	Koh	n.c	0.00	0.02	0.61	0.00	61	25	9	4	0	0.40	0.45	19.7	0.18	0.32
Voloshcha 1*	2870	J_2	Koh	0.92	0.02	n.c	0.68	0.00	63	22	10	5	0	0.53	0.57	5.48	0.44	0.40
Voloshcha 1*	2903	J_2	Koh	n.c	0.02	n.c	0.71	0.00	59	23	11	7	0	0.62	0.47	13.6	0.31	0.36
Korolyn 6	3642	J_1	Koh	3.13	0.06	n.c	0.66	0.54	51	26	13	7	3	0.49	0.13	24.6	0.53	1.00
Podiltsi 1*	3316	J_1	Koh	1.46	0.10	n.c	1.26	0.44	44	33	13	7	3	0.59	0.37	11.3	0.44	0.92
Voloshcha 1*	2952	J_1	Koh	1.39	0.04	n.c	0.99	0.38	49	27	13	8	3	0.53	0.49	26.9	0.42	0.57
Voloshcha 1*	3126	J_1	Koh	0.85	0.02	n.c	0.75	0.63	40	43	11	4	2	0.53	0.35	3.30	0.42	0.91
Korolyn 6	4157	J_1	Pod	0.27	0.05	n.c	0.66	0.98	38	25	16	11	10	0.36	0.06	84.8	0.18	1.00
Podiltsi 1	3475	J_1	Pod	0.27	0.03	n.c	1.02	0.66	49	24	13	8	6	0.48	0.18	91.3	0.15	0.95
Voloshcha 1	3370	J_1	Pod	0.68	0.04	n.c	0.58	0.85	38	24	17	12	10	0.53	0.13	24.1	0.32	0.73
Voloshcha 1	3547	J_1	Pod	0.41	0.07	n.c	0.64	0.89	36	25	17	12	10	0.43	0.03	22.2	0.19	0.91

Key: *Str* stratigraphy, J_2 Middle Jurassic, J_1 Lower Jurassic, *Form.* Formation, *Koh* Kokhanivka, *Pod* Podil'tsi, *Pr* pristane, *Ph* phytane, *Dia* diasterane, *Reg* regular sterane, *DBT* dibenzothiophene, *Phen* phenantrene, *GI* gammacerane index = Gam/$C_{30}H$ (Peters et al. 2005), *Gam* gammacerane, $C_{30}H$ C_{30} 17α(H)-hopane, $C_{29}H$ C_{29}Tm17α(H)21β(H)-norhopane, $C_{35}S$ C_{35}22S 17α(H) homohopane, $C_{34}S$ C_{34}22S 17α(H) homohopane, *Fl* fluoranthene, *Py* pyrene, *BaA* benz[a]anthracene, *Chr* triphenylene + chrysene, *PIR* (Cad + Sim + TDHA* + *ip*-*i*HMN + Fl + BaA + BaP + BgP + Cor)/(Cad + Sim + TDHA + *ip*-*i*HMN) (Zakrzewski and Kosakowski 2021); *LMW/Total* = (Phen + Ant + Fl + Py)/(Phen + Ant + Fl + Py + BaA + Chr + BkFl + BeP + BaP + IPy + BgP) (Karp et al. 2020); *BNF* benzo[b]naphtho[d]furans, *BgP* benzo[*ghi*]perylene, *Per* perylene, "+" present, *tr* traces, *n.c.* not calculated, *samples which PIR and LMW/total results were published in Zakrzewski and Kosakowski (2021). All depth values in metres. In our case total dehydroabietic acid (TDHA) = DAME

Discussion

There is a possibility that epigenetic processes (e.g. water washing) have affected the biomarker composition of the analysed rocks, resulting in the partial removal of e.g. short-chain *n*-alkanes, acyclic isoprenoids, and methyl- and dimethylnaphthalenes for example. A similar situation was reported in some Miocene coal samples from Poland (Fabiańska 2007). For this reason, conclusions based on ratios containing short-chain *n*-alkanes and/or acyclic isoprenoids are supported by other biomarker indicators, where epigenetic processes did not influence the results.

Hydrocarbon potential and facies

Rock-Eval pyrolysis allowed us to briefly describe the hydrocarbon potential of the Podil'tsi and Kokhanivka Fms. The Rock-Eval pyrolysis results obtained within the analysed samples show that both formations contain indigenous hydrocarbons (Fig. 4d) originating mostly from type III kerogen (Fig. 4a). The hydrocarbon content within the Podil'tsi Fm., as well as within the lower and upper parts of the Kokhanivka Fm., is generally poor (Figs. 4c, 5). The highest hydrocarbon content and TOC are observed in the middle part of the Kokhanivka Fm. (Fig. 5). This vertical variation of the hydrocarbon content and TOC can be noted in three boreholes: Korolyn 6, Podil'tsi 1, and Voloshcha 1 (Fig. 5). Due to an insufficient quantity of Rock-Eval pyrolysis analyses conducted in the Bortyatin 1 borehole the vertical variations of the TOC and hydrocarbon content within this borehole were not discussed.

Analysis of the Rock-Eval pyrolysis data allows us to conclude that the middle part of the Kokhanivka Fm. possesses fair-to-good hydrocarbon potential (Fig. 5). The rest of the Kokhanivka Fm. and all of the Podil'tsi Fm. are characterised by poor hydrocarbon potential.

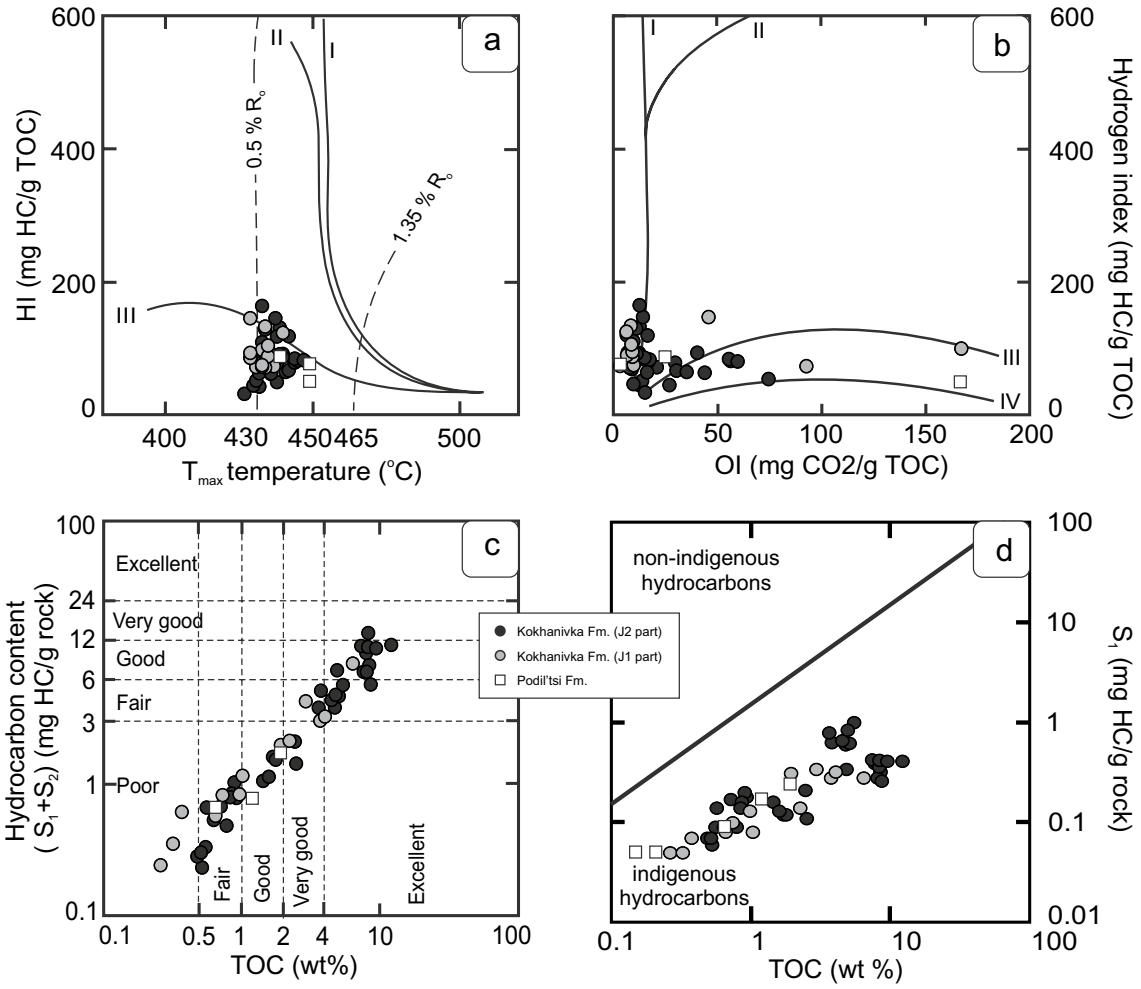

Fig. 4 Illustration of Rock-Eval results: **a** HI vs T_{max} plot, **b** HI vs OI plot; **c** hydrocarbon potential plot (after Peters and Cassa 1994); **d** origin of Lower Jurassic hydrocarbons shown on S_1/TOC plot

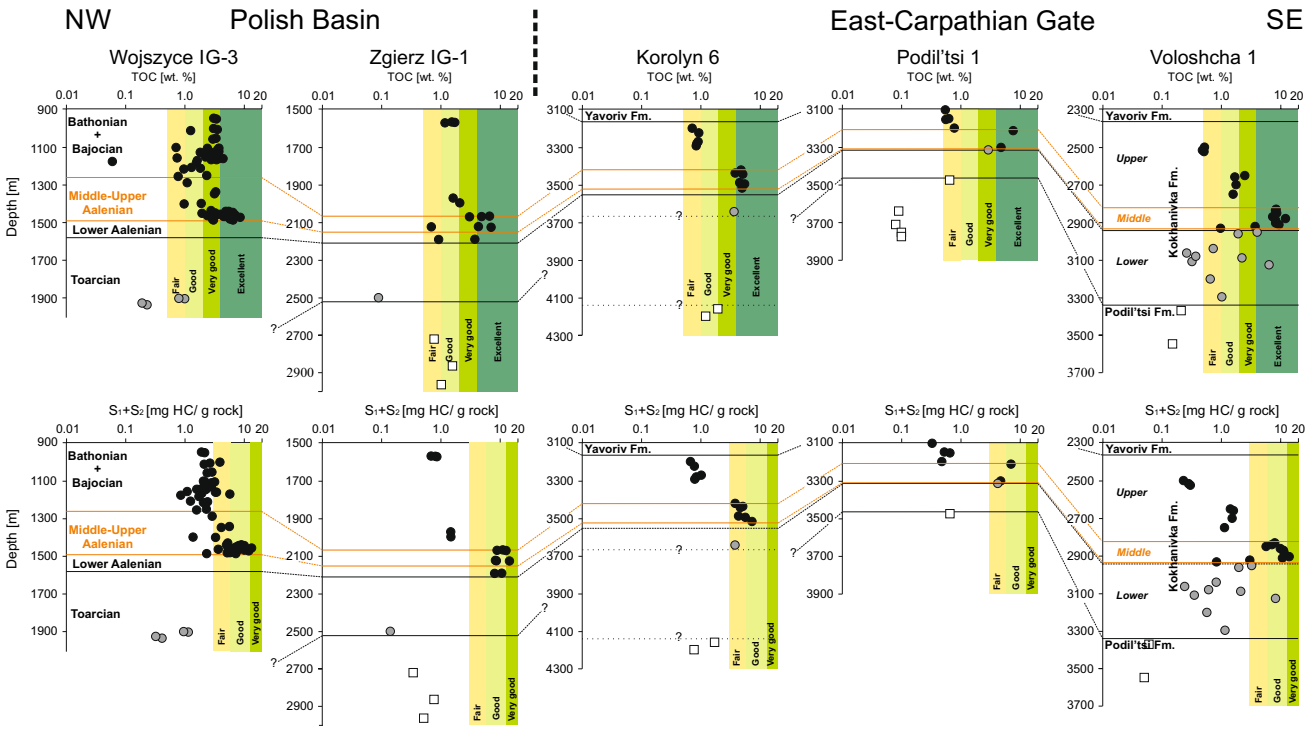

Fig. 5 Chemostratigraphical correlation based on vertical variability of TOC and S_1+S_2 across selected boreholes from the Polish Basin and East Carpathian Gate areas. Detailed Rock-Eval data for boreholes from Polish Basin were published in Zakrzewski et al. 2022a and b

Facies analysis revealed that in general, facies FT1-5 and part of the black claystones/mudstones related to FT6 are characterised by poor hydrocarbon potential and poor-to-fair TOC values. Higher hydrocarbon potential correlated with elevated TOC values was observed only within the brown claystones/mudstones classified to FT6 and single grey claystones intervals related to FT3 (Figs. 2, 5).

Organic matter maturity

The maturity of both formations was described in Kosakowski et al. (2012), so this subsection is not extensively developed. According to the obtained Rock-Eval pyrolysis as well as the biomarker indicator $C_{29}\beta\beta/(\alpha\alpha+\beta\beta)$, $C_{29}20S/(S+R)$, and $C_{31}S/(S+R)$ results, the Pliensbachian Podil'tsi Fm. contains mature organic matter (Table 2; Figs. 4a, 6).

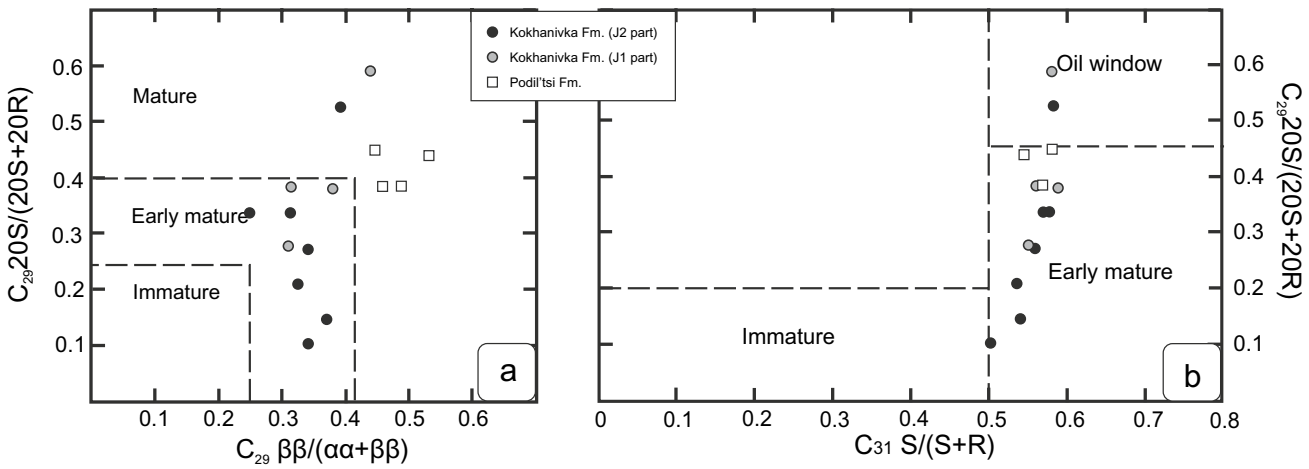

Fig. 6 Diagnostic plots of **a** C_{29} $\beta\beta/(\alpha\alpha+\beta\beta)$ versus C_{29} $20S/(S+R)$ and **b** C_{29} $20S/(S+R)$ versus C_{31} $20S/(S+R)$, describing organic matter maturity level (maturity fields after Peters and Moldowan 1993)

However, only a sample from the Korolyn 6 borehole probably exceeded 0.69%Ro as the perylene was not observed in the sample from the depth of 4157 m, despite the presence of other plant-derived aromatic biomarkers (Table 2) (Marynowski et al. 2015). The vitrinite reflectance values published by Kosakowski et al. (2012) partially support the maturity level of the Podil'tsi Fm. suggested by the biomarkers. However, a very high Ro value obtained within the Voloshcha 1/3547 sample in our opinion might be linked with redeposited organic matter, as this sample contains perylene (Table 2). In the Podil'tsi 1 and Voloshcha 1 boreholes, the analysed Podil'tsi Fm. contains early-mature organic matter in the range of 0.61–0.69%Ro. In the Korolyn 6 borehole, the Podil'tsi Fm. exceeded 0.69%Ro but did not reach 0.90%Ro as the BaP is present in all the samples from this borehole (Marynowski et al. 2015).

Calculated biomarker and Rock-Eval pyrolysis indicators suggest that the Kokhanivka Fm. contains mostly early-mature organic matter (Figs. 4a, 6). Only two samples from the Korolyn 6 borehole referred to the Kokhanivka Fm. are in the mature zone, but simultaneously the Middle Jurassic sample contains perylene, which suggests that in this case the Ro did not exceed 0.69% (Marynowski et al. 2015).

Origin of organic matter

According to the HI and T_{max} values, both the Podil'tsi and Kokhanivka Fms. contain mostly terrigenous type III kerogen (Fig. 4a). Some samples from brown claystones of the Kokhanivka Fm. contain a more significant admixture of sapropelic type II kerogen, which is suggested by higher HI results (Table 1; Fig. 4a). These preliminary conclusions were developed by the GC–MS results.

The distribution of *n*-alkanes within the analysed Lower–Middle Jurassic strata possesses a unimodal character. The Pliensbachian Podil'tsi Fm. is characterised by the domination of short-chain homologues linked with marine organic matter (Fig. 3c–d) (Bray and Evans 1961; Peters et al. 2005). This domination of short-chain homologues is reflected in the LTS_{HC} ratio results, which in most of the samples from the Podil'tsi Fm. are below 1, thus suggesting mostly marine organic matter origin (Kotarba et al. 2011a). A slightly higher admixture of terrestrial organic matter is noted in the sample Podil'tsi 1/3475, where LTS_{HC} is above 1 (Table 3). The Pr/C_{17} and Ph/C_{18} results suggest that the Podil'tsi Fm. contains mixed organic matter (Fig. 7b).

N-alkanes obtained within the Kokhanivka Fm. were dominated by mid-chain C_{21}–C_{25} homologues, which can be linked with aquatic plants, bryophytes, or phytoplankton (Table 3; Fig. 3b) (Ficken et al. 2000; Pancost et al. 2002; Mead et al. 2005; Chen et al. 2021). Only the lowermost part of the Kokhanivka Fm. is mostly characterised by the highest abundances of long-chain C_{27} homologue linked primarily with terrestrial plant input (Table 3; Fig. 3a) (Bray and Evans 1961; Peters et al. 2005). In the Korolyn 6 borehole area, we noted that the sample from the lower part of the Kokhanivka Fm. contains significant abundances of short-chain *n*-alkanes, which suggest a significant role of marine organic matter.

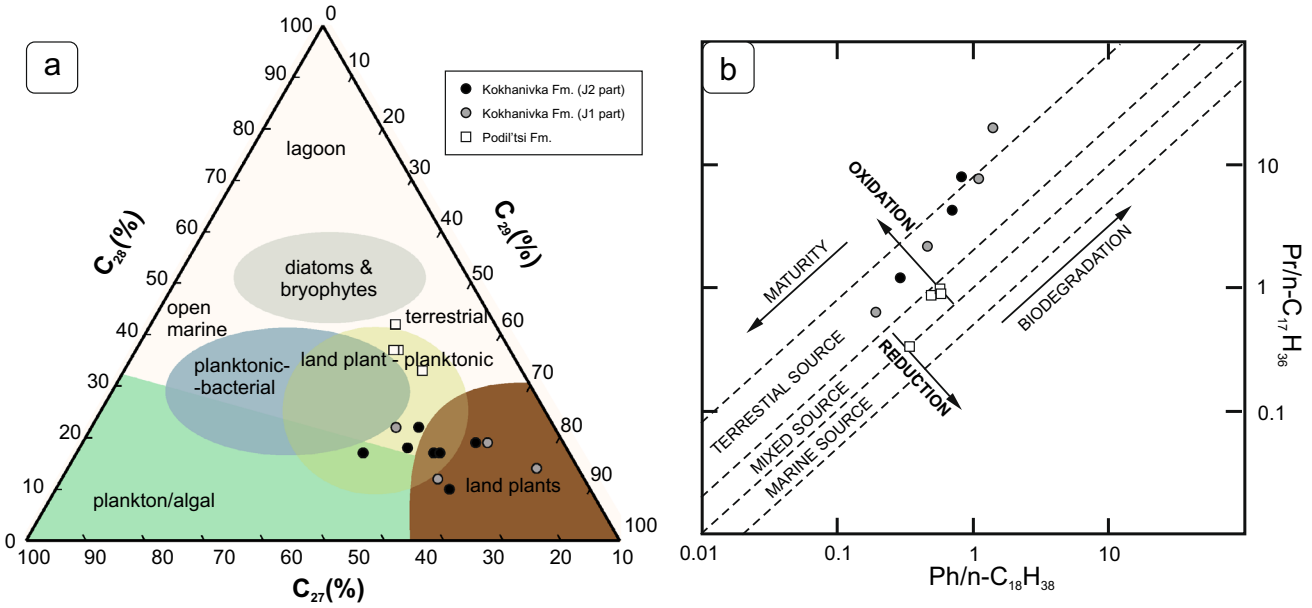

Fig. 7 **a** Ternary plot of regular steranes distribution within Podil'tsi and Kokhanivka Fms. (as normalised percentages; after Huang and Meinschein 1979; classification after Peters et al. 2005, modified). **b** Organic matter origin and maturity illustrated on $Pr/n\text{-}C_{17}$ vs $Ph/n\text{-}C_{18}$ plot (after Shanmugam 1985, modified)

Higher terrestrial input within the Kokhanivka Fm. is noted in the LTS_{HC} results, which in almost all cases extensively exceed 1 (Table 3). Also, Pr/C_{17} and Ph/C_{18} suggest the mostly terrestrial character of the organic matter within the Kokhanivka Fm. (Fig. 7b). The high Pr/C_{17} results within this formation should be linked with the case where pristane originates from tocopherols, which could come from land plants (Goossens et al. 1984; Peters et al. 2005). Similarly, elevated Pr/C_{17} values were observed within the Middle Jurassic of the PB, where significant terrestrial organic matter input was observed (Zakrzewski et al. 2020, 2022a).

General information taken from *n*-alkanes was developed by the application of other biomarkers. Regular sterane distribution suggests that the Podil'tsi Fm. contains mixed planktonic–land plant organic matter (Figs. 7a, 8a). This indicator confirms that the Kokhanivka Fm. contains mostly terrigenous organic matter with a minor role of planktonic organic matter (Figs. 7a, 8c). The high content of stigmastanes might be linked with green algae and/or terrigenous organic matter (Volkman 2003; Peters et al. 2005). However, our S/H results suggest mostly terrigenous origin of C_{29} steranes.

According to the low S/H results, the planktonic organic matter within both the Podil'tsi and Kokhanivka Fms. have mostly bacterial origin (Table 3). Results above 1 indicate the advantage of algae over bacterial input, as steranes are linked with algal input and hopanes are linked with bacterial input (Brooks 1970; Seifert and Moldowan 1979; Moldowan et al. 1985; Peters et al. 2005). The presence of the Cyanobacteria within the Podil'tsi Fm. and within part of the Kokhanivka Fm. samples was noted as the 7- and 8-MMA were marked (Table 3; Fig. 9B) (Klomp 1986; Fowler and Douglas 1987; Shiea et al. 1990). However, it is worth noting that these MMA were not observed within the Kokhanivka Fm. from the Podil'tsi 1 and Voloshcha 1 boreholes. Sulphur-reducing bacteria within the photic zone were noted mostly in the Podil'tsi Fm., where the presence of isorenieratane and renieratane were marked, suggesting the presence of

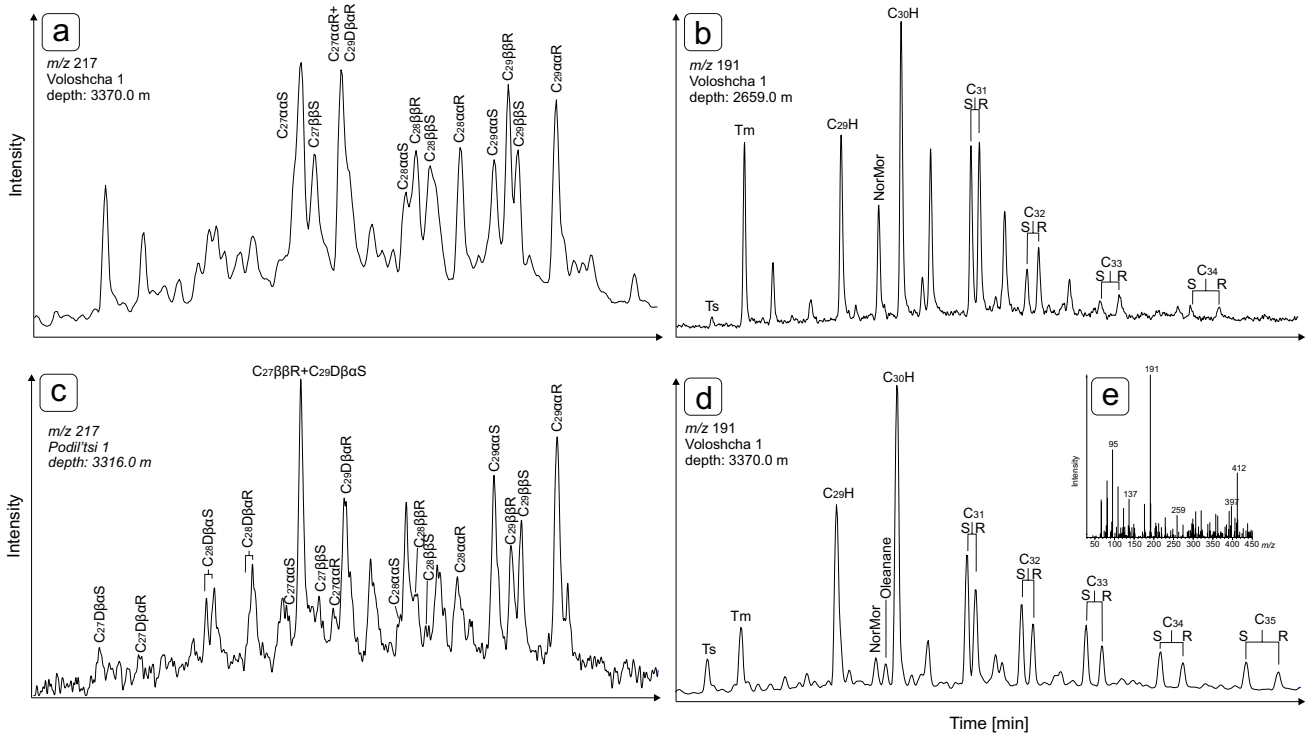

Fig. 8 Partial mass chromatograms of *m/z* 217 ion fragmentogram with steranes distribution within the sample from **a** Podil'tsi Fm and **c** Kokhanivka Fm. Partial mass chromatograms of *m/z* 191 ion fragmentogram with main pentacyclic terpane distribution obtained in **b** sample from Kokhanivka Fm. and **d** sample from Podil'tsi Fm. with **e** mass spectrum of oleanane from Podil'tsi Fm. **Key**: C_{27} DβαS—C_{27}βα20S diacholestane; C_{27} DβαR—C_{27}βα20R diacholestane; C_{26}ααR—C_{26}αα20R 24-norcholestane; C_{28} DβαS—C_{28}βα20S diacholestane; C_{28} DβαR—C_{28}βα20R diacholestane; C_{27}ααS—C_{27}αα20S cholestane; C_{27}ββR—C_{27}ββ20R cholestane; C_{29} DβαS—C_{29}βα20S diacholestane; C_{27}ββS—C_{27}ββ20S cholestane; C_{27}ααR—C_{27}αα20R cholestane; C_{29} DβαR—C_{29}βα20R diacholestane; C_{28}ααS—C_{28}αα20S ergostane; C_{28}ββR—C_{28}ββ20R ergostane; C_{28}ββS—C_{28}ββ20S ergostane; C_{28}ααR—C_{28}αα20R ergostane; C_{29}ααS—C_{29}αα20S stigmastane; C_{29}ββR—C_{29}ββ20R stigmastane; C_{29}ββS—C_{29}ββ20S stigmastane; C_{29}ααR—C_{29}αα20R stigmastane; *Ts* Ts 18a(H)-trisnorhopane, *Tm* Tm 17a(H)-trisnorhopane, C_{29}H—C_{29}Tm17α(H)21β(H)-norhopane; Normor—C_{29} normoretane; C_{30}H—C_{30} 17α(H)-hopane; C_{31}S—C_{31}22S 17α(H) homohopane; C_{31}R—C_{31}22R 17α(H) homohopane; Gam—Gammacerane; C_{32}S—C_{32}22S 17α(H) homohopane; C_{32}R—C_{32}22R 17α(H) homohopane; C_{33}S—C_{33}22S 17α(H) homohopane; C_{33}R—C_{33}22R 17α(H) homohopane; C_{34}S—C_{34}22S 17α(H) homohopane; C_{34}R—C_{34}22R 17α(H) homohopane, C_{35}S—C_{35}22S 17α(H) homohopane; C_{35}R—C_{35}22R 17α(H) homohopane

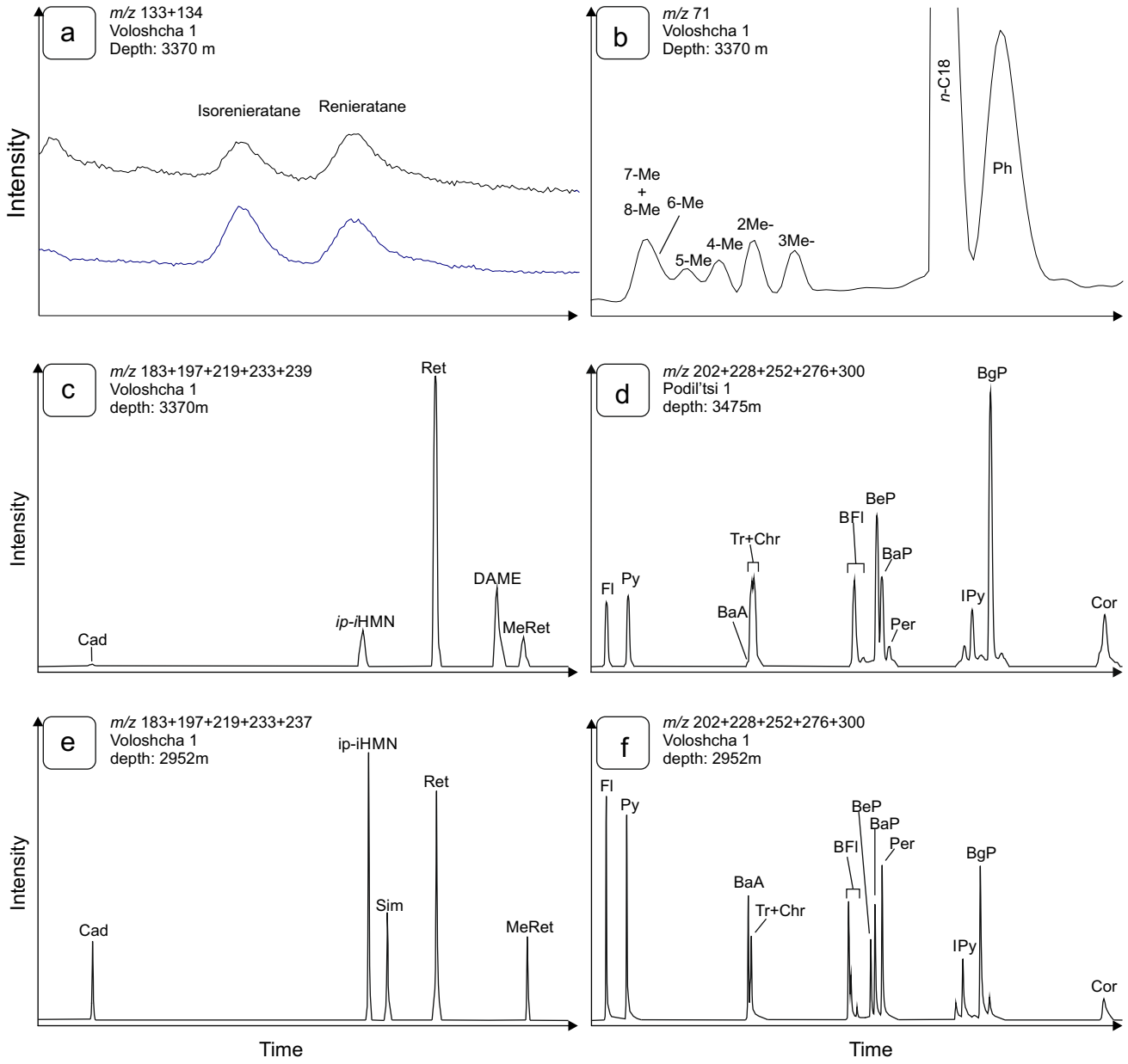

Fig. 9 **a** Distribution of C_{40} aromatic carotenoids, and **b** MMA within Podil'tsi Fm; **c, e** main plant-derived aromatic biomarkers marked in analysed samples; **d, f** typical PAHs distribution within Podil'tsi and Kokhanivka Fms. **Key:** *Cad* cadalene, *Ret* retene, *Sim* simonellite, *ip-iHMN* 6-isopropyl,1-isohexyl,2-methylnapthaplene, *DAME* dehydrabietic acid methyl ester, *MeRet* 2-methylretene, *Fl* fluoranthene, *Py* pyrene, *BaA* benzo[a]anthracene, *Tr + Chr* triphenylene and chrysene, *BFl* benzofluoranthenes, *BeP* benzo[*e*]pyrene, *BaP* benzo[*α*]pyrene, *Per* perylene, *IPy* indeno(1,2,3,cd-)pyrene, *BgP* benzo[*ghi*]perylene, *Cor* coronene

brown- and green-pigmented Chlorobiaceae (Table 4; Fig. 9A) (Brocks and Schaeffer 2008). Within the Kokhanivka Fm., a minor abundance of renieratane was observed only within one sample that referred to the lower part of the formation (Table 4). Cui et al. (2020) also suggest the cyanobacterial origin of isorenieratane and renieratane but in our cases, the C_{38} and C_{39} aromatic carotenoids are absent or present in minor abundances, which suggests that the aromatic carotenoids originated primarily from sulphur-reducing bacteria.

Besides the aliphatic diterpanes, only the 16a-phyllocladane and abietane were noted within the Podil'tsi Fm. (Table 3). The presence of 16a-phyllocladane suggests the occurrence of conifers other than Pinaceae in the sediment supply area (e.g. Otto and Simoneit 2002). However, it is worth noting that all samples from the Podil'tsi Fm. also contain oleanane, which is commonly linked with angiosperms (Table 3; Fig. 8d–e) (Peters et al. 2005, and references therein). Oleanane presence within the Lower Jurassic

strata is unexpected, but to date this compound was revealed within the Middle Jurassic, Permian, and Carboniferous strata (Moldowan et al. 1994; Taylor et al. 2006; Philp et al. 2021). Taylor et al. (2006) suggest oleanane presence within fossilised Cretaceous Bennettitales and Permian Gigantopterids. The Bennettitales were present within Early Jurassic flora (e.g. Popa and Zaharia 2011), so the oleananes within the Podil'tsi Fm. might be linked with this type of plant. Low content of free hydrocarbons versus TOC suggests that oleanane has an indigenous origin and should not be linked with hydrocarbon migration from younger horizons (Fig. 4d). Despite the significant input of terrestrial organic matter within the Kokhanivka Fm., aliphatic diterpanes are rarely reported and their restricted presence was noted only within the lower part of this formation related to the Toarcian–Lower Aalenian strata (Table 3).

Despite the rare occurrence of aliphatic diterpanes, all analysed samples contained plant-derived aromatic biomarkers, which are partially aromatic products of diterpenes (Simoneit 1977; Alexander et al. 1986; Ellis 1994; Fabiańska 2007). The marking of retene, cadalene, *ip*-*i*HMN, and perylene (Tables 2, 4) suggests the presence of conifers, bryophytes, and fungi (van Aarssen et al. 2000; Hautevelle et al. 2006; Romero-Sarmiento et al. 2011; Marynowski et al. 2013; Cesar and Grice 2019). The most common compounds are retene and *ip*-*i*HMN that are linked mostly with conifers and bryophytes, respectively (van Aarssen et al. 2000; Cesar and Grice 2019). Cadalene, which besides conifers might be linked for example with coastal vegetation (Cesar and Grice 2019), was present in most of the Lower–Middle Jurassic samples, but in relatively low abundances in comparison to retene and *ip*-*i*HMN, which was noticeable during the analysis of the plant fingerprint (PF) (Table 4.; Fig. 9c, e). The PF in most samples is dominated by retene. The higher values of cadalene (> 2% in PF) were observed only within the lowermost Kokhanivka Fm., related probably to the Toarcian Age (Table 4; Fig. 9e). This part of the Kokhanivka Fm. is also frequently characterised by the highest content of *ip*-*i*HMN within PF (Table 4), which reflects the changes within the palaeoflora (Cesar and Grice 2019). The retene diagenetic precursors (e.g. simonellite and methylretene) were marked only within the Kokhanivka Fm. The absence of these compounds within the Podil'tsi Fm. suggests that retene from this formation might be from the redeposition of older and more mature horizons, or was formed during palaeo-wildfire events (Ruebsam et al. 2020; Zakrzewski et al. 2020, 2022a).

The lack or minor role of aliphatic diterpanes, together with the common presence of diterpenoid aromatic derivatives, suggest that the Lower–Middle Jurassic strata contain mostly oxidised terrestrial organic matter and/or terrigenous organic matter where conifers were not the dominating type of plants (Simoneit 2005; Fabiańska 2007). This oxidation could take place during reported palaeo-wildfires events, such as in the Lower–Middle Jurassic strata in the nearby PB (Zakrzewski et al. 2020, 2022a, b). This explains why cadalene is present only in minimal abundance, as this compound is vulnerable to thermal degradationthat can occur during palaeo-wildfire events (Izart et al. 2012; Zakrzewski and Kosakowski 2021). The results of PIR suggest that palaeo-wildfire events had a place in the sediment supply area, but the scale of the pyrolytic residue input was lower than in the central part of the PB area (Table 6). Mostly, the pyrolytic origin of PAHs demonstrated by Fl/(Fl + Py) and BaA/(BaA + Chr) for the Kokhanivka Fm. also supports the thesis about at least the partial pyrolytic origin of retene (Table 5; Figs. 9f, 10b). The presence of diagenetic precursors of retene like simonellite and methylretene indicate that other parts of retene have a diagenetic origin (Table 4; Fig. 9c, e). The rate of diagenetic precursors of retene versus retene increased in samples with a higher presence of *ip*-*i*HMN versus retene (Table 4; Fig. 10f). Elevated content of *ip*-*i*HMN, frequently linked with bryophytes might suggest more humid palaeoclimate conditions (Cesar and Grice 2019). A good correlation between the content of the diagenetic precursors of retene and *ip*-*i*HMN versus retene indicates that the rate of pyrogenic versus diagenetic origin retene decreased in more humid palaeoclimate conditions (Fig. 10f).

Within the Podil'tsi Fm., the PAHs have mostly petrogenic origin (sensu Yunker et al. 2002) (Table 5; Figs. 9d, 10b). In this formation besides the diagenetic processes, the plant-derived aromatic biomarkers might come from the redeposition of older organic-rich deposits, such as Carboniferous coals, which were postulated for Toarcian sediments from the southern part of the PB (Ruebsam et al. 2020).

Most of the Lower–Middle Jurassic samples contain significant amounts of perylene (Table 2; Fig. 9d, f). Perylene is commonly linked with fungi and might be evidence of palaeoestuaries located near sampled boreholes (Marynowski et al. 2013; Varnosfaderany et al. 2014). The role of these palaeoestuaries in sediment transport was significant within the Kokhanivka Fm. samples, where the significant input of terrestrial organic matter was noted (Tables 4, 5; Figs. 7, 9c, e). Even in more marine samples representing the Podil'tsi Fm., the terrestrial organic matter input can be noted as the perylene is present in deposits representing this formation (Table 2). Only within the Lower Jurassic samples from the Korolyn 6 borehole, is the perylene absent, but this absence is probably linked with thermal maturity (Marynowski et al. 2015).

Palaeoenvironmental conditions

Combined biomarker and sedimentological results were used to define the palaeoenvironmental conditions. Based on the biomarkers from the aliphatic and aromatic fractions, the

Table 6 Generalised chemostratigraphic characteristics of Toarcian–Bathonian strata from the Polish Basin and East Carpathian Gate areas

Location	Age	Lithology	TOC	S_1+S_2	OM origin	H. *n*-alkanes	Diterpanes	Average PF			Palaeowildfires intensity	PAHs	Homohopane index	DBT/Phen
								Cad	Ret	*ip-i*HMN				
Polish Basin	Bajocian–Bathonian	Hetherolith (sandstones with dark claystones/mudstones layers)	Good	Poor	Mixed (terrestrial > marine)	25–27 or 18–20	Rare	11	82	7	High Avg. PIR = 120	Mostly pyrogenic, mostly residue origin	0–10	< 0.20
	Middle–Upper Aalenian	Dark grey to black claystones/mudstones	Excellent	Fair/good	Mostly terrestrial	23	Rare	7	82	11	High/moderate Avg. PIR = 81	Mostly pyrogenic, mixed smoke/residue origin	1–10	< 0.20
	Toarcian	Sandstones with mudstone/claystone layers	Fair/good	Poor	Mostly terrestrial	23–27	Present	1	90	9	Moderate Avg. PIR = 47	Mixed, residue origin	2–3	< 0.20
ECG	Bajocian–Bathonian	Dark grey, black claystones	Fair/good	Poor	Mostly terrestrial	25	Absent	0	95	5	Moderate Avg. PIR = 20	Mostly pyrogenic, residue origin	0	< 0.20
	Middle–Upper Aalenian	Brown to black claystones/mudstones	Excellent	Fair/good	Mostly terrestrial	23	Absent	1	90	9	Moderate Avg. PIR = 20	Mostly pyrogenic, mixed smoke/residue origin	0–3	< 0.20
	Toarcian	Dark grey claystones (Kokhanivka Fm.) or sandstones (Medenychi Fm.)	Fair/good	Poor	Mostly terrestrial	25–27	Present	12	62	26	Moderate/low Avg. PIR = 17	Mostly pyrogenic, mostly smoke origin	2–3	< 0.20

Key: *ECG* East Carpathian Gate, *OM* organic matter, *H. n-alkanes n*-alkanes with the highest abundance, *Average PF* average values of Cad, Ret, and *ip-i*HMN calculated as an average value from data referred to each age and location. For example to obtain the Average Cad value for the Toarcian horizon from the Polish Basin, we calculated average values from Toarcian samples published by Zakrzewski et al. (2022b); homohopane index – 100*(C_{35} homohopane/Σ C_{31}–C_{35} homohopanes) (Peters et al. 2005, and references therein)

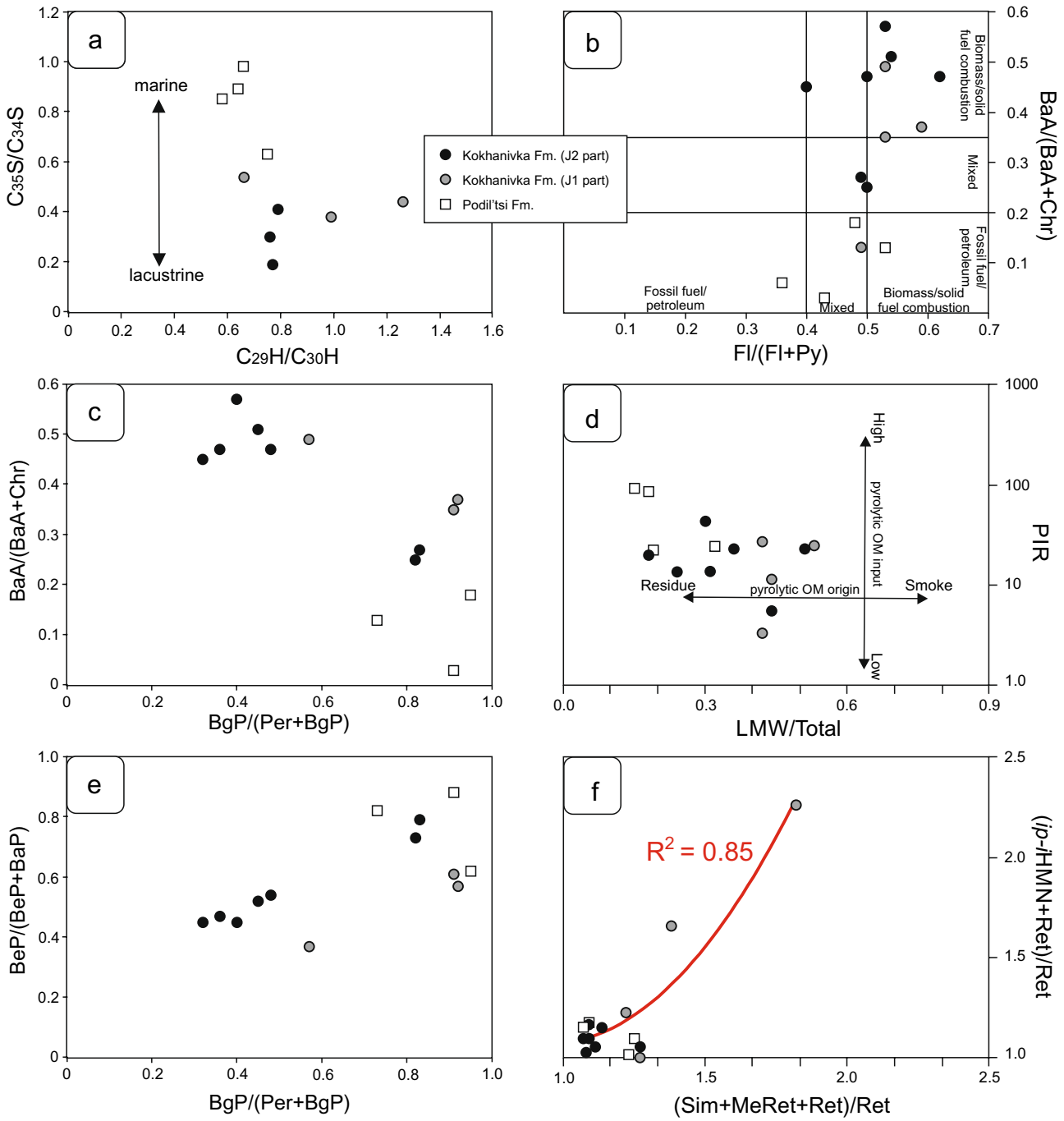

Fig. 10 Set of plots characterising palaeoenvironmental conditions during deposition: **a** $C_{35}S/C_{34}S$ vs $C_{29}H/C_{30}H$ plot (after Peters et al. 2005); **b** Fl/(Fl + Py) vs BaA/(BaA + Chr) plot (after Yunker et al. 2002); **c** BaA/(BaA + Chr) vs BgP/(Per + BgP) (this study); **d** PIR vs LMW/total plot (after Zakrzewski and Kosakowski 2021); **e** BeP/(BeP + BaP) vs BgP/(Per + BgP) (this study); **f** (*ip*-*i*HMN + Ret)/Ret vs (Sim + MeRet + Ret)/Ret (this study). Abbreviations as in Tables 3, 4, and 5

redox conditions in the photic zone and at the basement were described. Furthermore, information about, palaeo-wildfires, and palaeogeography is included in this subsection.

In the study area, during the Hettangian–Sinemurian Age the sedimentation took place in the basin opened to the south direction and simultaneously separated from the neighbouring PB (Feldman-Olszewska 1997; Pieńkowski 2004). Sedimentation probably occurred under the conditions of rapid subsidence of the bottom of a tectonic graben (Ovcharenko et al. 1999; Dulub et al. 2003; Karpenchuk et al. 2006). During the Pliensbachian, sedimentation took place under lagoonal conditions with intermittent open

sea connections (FT 1, 2) (Świdrowska et al. 2008). In the lower part of the Toarcian–Aalenian siliciclastic succession, there was a decreasing amount of plant debris and periodically developing shallow-water bioclastic limestones forming thin intercalations. The mosaic pattern of lithofacies featured in adjacent boreholes' distribution may indicate deltaic, tidal plain, and lacustrine–estuarine environments with increasing marine influence (FT 3, 4) (Gareckij 1985; Świdrowska et al. 2008). A typical marine environment of shallow siliciclastic shelf prevailed during the Bajocian and Bathonian periods (FT 5, 6). The fauna indicates a rather stable open marine environment (e.g. Dulub et al. 2003; Zhabina et al. 2017).

Unfortunately, secondary processes caused situations where Pr and Ph were not detected in some samples. For this reason, the Pr/Ph ratio was not calculated within four samples from the Kokhanivka Fm., as the Pr and/or Ph were not marked in these samples (Table 5). The obtained Pr/Ph results within the Lower–Middle Jurassic strata suggest mostly dysoxic and anoxic conditions in the basement (Didyk et al. 1978; Peters et al. 2005). However, it must be noted that the Pr/Ph ratio has many limitations linked with maturity and organic matter's origin. Pr/Ph is vulnerable, for example, to high terrestrial organic matter input, which might overestimate the Pr/Ph results as Pr can be derived from tocopherols (Goossens et al. 1984; Peters et al. 2005). On the other hand, Ph abundance might be boosted by halophilic bacteria (Ten Haven et al. 1987; Peters et al. 2005). The Pr/Ph values generally increase with increasing thermal maturity of the organic matter. This phenomenon is mainly controlled by more Pr precursors in the source kerogens (Koopmans et al. 1999; Peters et al. 2005, and references therein). For these reasons, the Pr/Ph results were supported by homohopane distribution (Table 5). Broad C_{31}–C_{35} homohopane distribution with fair C_{33} and C_{34} homologues content support the statement about the suboxic/dysoxic conditions during the deposition of the Lower–Middle Jurassic strata (Demaison et al. 1983; Obermajer et al. 2000; Peters et al. 2005). According to the obtained results, the Podil'tsi Fm. was deposited under dysoxic conditions. Within the Kokhanivka Fm., the C_{33}–C_{35} homologues' content within the homohopane distribution is lower, which suggests suboxic conditions during deposition. The scarcity of oxygen during the deposition of both analysed formations is also suggested by the presence of pyrite, whose occurrence was described by Kosakowski et al. (2012) and Rauball et al. (2020).

During the deposition of the Kokhanivka Fm., within the photic zone, the domination of oxic conditions was recorded as aromatic carotenoids (e.g. isorenieratane and renieratane), diaryl isoprenoids, and aryl isoprenoids were not detected in all but one sample (Schwark and Frimmel 2004; Brocks and Schaeffer 2008). Different redox conditions were noted in the Podil'tsi Fm., where the presence of isorenieratane and renieratane indicate the scarcity of oxygen within the photic zone (Table 4). A combination of information about the redox conditions suggests that the Podil'tsi and Kokhanivka Fms. might be deposited in shallow-marine environments (< 200 m depth) where the photic zone reached the basement as the redox conditions in the entire water column are similar (Tables 5, 6). The obtained $C_{29}H/C_{30}H$ versus $C_{35}S/C_{34}S$ support the suggestion that the Podil'tsi Fm. was deposited in more marine palaeoenvironment than the Kokhanivka Fm. (Fig. 10a) (Peters et al. 2005).

The lack of gammacerane suggests that these formations were deposited in brackish-to-normal saline marine environments (e.g. Wang et al. 2022, and references therein). Moreover, the low (< 0.10) gammacerane index together with low (< 0.10) DBT/Phen values suggest that the deposition of both Fms. took place in iron-rich and non-sulphidic conditions where pyrite was formed in the water column (Table 5). A similar situation was observed in Lower Jurassic deposits from the West Netherlands and West Cleveland Basins, where reactive iron was also supplied by terrigenous input (de Leeuw and Sinninghe-Damsté 1990; Sinninghe Damsté et al. 1995; Song et al. 2017).

All analysed samples contain a series of > 5-ring PAHs, which might be linked with palaeo-wildfires (e.g. Marynowski and Simoneit 2009). The origin of PAHs was described based on the Fl/(Fl + Py) versus BaA/(BaA + Chr) diagnostic plot (Fig. 10b) (Yunker et al. 2002; Xu et al. 2019). This plot indicates that PAHs from the Kokhanivka Fm. have mostly pyrogenic origin. A more significant influence of petrogenic PAHs within the Kokhanivka Fm. was noted only within samples from the Korolyn 6 borehole, which are characterised by the highest maturity (Tables 2, 5; Fig. 10b). In the case of the Podil'tsi Fm., the PAHs have mostly petrogenic origin (Fig. 10b). Most of the samples from the Kokhanivka Fm. were described in Zakrzewski and Kosakowski's (2021) study, but it must be noted that Zakrzewski and Kosakowski (2021) based their analyses on obsolete stratigraphical identification drawn from Kosakowski et al. (2012).

LMW/total and PIR indicators were used to describe the origin and rate of pyrolytic organic matter within the analysed samples (Table 5). Part of this data was used by Zakrzewski and Kosakowski (2021); nevertheless, we include them in this paper because of the stratigraphical changes in the borehole Voloshcha 1 in comparison to the stratigraphy used in Kosakowski et al. (2012) and Zakrzewski and Kosakowski (2021). According to the PIR and LMW/Total results, the influx of pyrolytic organic matter during the deposition of the Kokhanivka Fm. was less than in the same period in the PB area, as the PIR values are lower in comparison to those obtained from the Middle Jurassic strata from the PB (Table 6) (Zakrzewski and Kosakowski 2021; Zakrzewski et al. 2022a). Moreover, the higher LMW/Total results suggest the more significant participation of smoke-origin PAHs in comparison to the Middle Jurassic strata from the PB. In the upper part of the Kokhanivka Fm., the participation of smoke-origin PAHs decreased as the

LMW/Total results also decreased (Table 5; Fig. 10d) (Karp et al. 2020; Zakrzewski and Kosakowski 2021).

The lower input of pyrolytic residues in samples within the Kokhanivka Fm. was controlled by palaeogeography, which is suggested by two plots juxtaposing BaA/(BaA + Chr) and BeP/(BeP + BaP) versus BgP/(Per + BgP) (Fig. 10c, e). This conclusion is based on the statement that perylene is linked with fungi and might be used as an indicator of distance from palaeoestuaries (Marynowski et al. 2013; Varnosfaderany et al. 2014; Zakrzewski et al. 2020). The BgP/(Per + BgP) indicator was used to approximately characterise the palaeogeographical differences between the analysed samples, as BgP/(Per + BgP) results below 0.5 should be interpreted as conditions with a significant influence of palaeoestuaries (Zakrzewski et al. 2020). The BaA/(BaA + Chr) versus BgP/(Per + BgP) plot revealed that samples from the Kokhanivka Fm. with a high influence of palaeoestuaries are characterised by the presence of mostly pyrogenic PAHs, as BaA/(BaA + Chr) reached the highest values within these samples (Table 5; Fig. 10c). Similar conclusions can be taken from BeP/(BeP + BaP) versus BgP/(Per + BgP), as the BeP/(BeP + BaP) can be used to distinguish samples with a higher influence of phytoplankton (Fig. 10e) (Grice et al. 2007). Therefore, samples with the highest influence of phytoplankton are characterised by the least influence of palaeoestuaries. A combination of data obtained from the dependencies described above allows us to state that the lowermost Kokhanivka Fm. from the Podil'tsi 1 and Voloshcha 1 boreholes as well as the Kokhanivka Fm. from Korolyn 6 were deposited in the far distance and are characterised by a low influence of palaeoestuaries. Other samples from the Kokhanivka Fm. were deposited under a moderate-to-significant influence of palaeoestuaries.

BgP/(Per + BgP) should be used in samples with mostly immature to early-mature terrigenous organic matter. Perylene disappeared from the samples when the thermal maturity of Ro = 0.69% is exceeded, but above Ro = 0.60% the perylene abundance decreased, leading to an overestimation of BgP/(Per + BgP) (Marynowski et al. 2015; Zakrzewski et al. 2020). Due to the high maturity and/or mostly marine organic matter origin, the results of the Podil'tsi Fm. presented on plots with the BgP/(Per + BgP) ratio should be interpreted with caution (Fig. 10c, e).

Chemostratigraphic correlation between the Middle Jurassic of the East Carpathian Gate and Polish Basin areas

Analysis of the obtained Rock-Eval pyrolysis and biomarker results allow us to characterise the Podil'tsi and Kokhanivka Fms. Moreover, during the interpretation of these results, we matched the chemostratigraphic correlation between these formations and the same aged horizons from the PB.

Analysis of the Rock-Eval pyrolysis data shows that from the analysed Podil'tsi and Kokhanivka Fms., only the middle part of the Kokhanivka Fm. possesses fair-to-good hydrocarbon potential while the rest of the described Fms. is characterised by poor hydrocarbon potential (Table 6; Fig. 5). A similar situation was noted in the Lower-to-Middle Jurassic strata from the PB, where only the Middle–Upper Aalenian strata are characterised by fair-to-good hydrocarbon potential (Zakrzewski et al. 2022a, b). In the PB area, the rest of the Lower and Middle Jurassic strata shows poor hydrocarbon potential (Zakrzewski et al. 2022a, b). Besides hydrocarbon potential, elevated TOC results were also observed within the middle part of the Kokhanivka Fm and Middle–Upper Aalenian strata from the PB (Fig. 5). The detailed localisation of the boreholes from Fig. 5 is presented in Fig. 1D.

The next portion of geochemical similarities in the Toarcian-to-Bathonian strata from the ECG and PB were determined by biomarker distribution (Table 6).

The *n*-alkanes' distribution in both areas is mostly dominated by mid- and long-chain homologues. Within the Toarcian strata, the extensive role of the *n*-C_{27} homologue within the *n*-alkanes' distribution was marked in the PB and ECG areas. The mid-chain *n*-C_{23} homologue reached the highest abundances within the Middle–Upper Aalenian strata from the PB, and within the middle Kokhanivka Fm. from the ECG area. A slightly more complicated situation was noted within the Bajocian–Bathonian strata, which is related to the expansion of the PB and the variability of the organic matter's origin (Zakrzewski et al. 2022a). However, even within the Bajocian–Bathonian strata, the similarities between the PB and ECG are noted, as the *n*-C_{23} is no longer the most abundant *n*-alkane and the highest peaks moved towards the *n*-C_{25} homologue (Table 6).

Despite the significant input of terrestrial organic matter noted within the Kokhanivka Fm., aliphatic diterpanes are rare findings and their limited occurrence was noted only within the lower part of this formation related to the Toarcian–Lower Aalenian strata (Tables 3, 6). A similar limitation of aliphatic diterpanes distribution was noted within the Middle Jurassic strata from the PB, where terrigenous organic matter was oxidised during palaeo-wildfire events (Zakrzewski et al. 2022a). Furthermore, the Lower Jurassic strata from the PB, which in comparison to the Middle Jurassic strata were less influenced by palaeo-wildfires, contain aliphatic diterpanes (Zakrzewski et al. 2022b), thus supporting the claim that analysed samples from the lower part of the Kokhanivka Fm. might be related to the Toarcian Age (Table 6).

Finally, the similarities between the PB and ECG were noted in the distribution of palaeo-wildfire indicators, which suggest that in general the intensity of palaeo-wildfires and the prevalence of pyrolytic residue versus smoke-origin PAHs rises from the Toarcian towards the

Bajocian–Bathonian strata (Table 6). Moreover, the palaeoenvironmental conditions during the deposition of the Toarcian–Bathonian strata from the PB and ECG were similar, as these strata in both areas were deposited in suboxic-to-dysoxic and sulphate-poor conditions (Table 6).

As described above, the similarities in the Rock-Eval pyrolysis results and similar trends observed within the biomarkers gathered in Table 6 support the claim that the middle part of the Kokhanivka Fm. is related to the Middle–Upper Aalenian strata from the PB.

Conclusions

1. The Lower–Middle Jurassic strata in general contain mixed organic matter. Within the Pliensbachian Podil'tsi Fm., the prevalence of marine organic matter was noted. The significant input of terrigenous organic matter was noted within the Toarcian–Bathonian Kokhanivka Fm.
2. The Phytoplankton was dominated by bacteria. Traces of cyanobacteria as well as green- and brown-pigmented Chlorobiaceae were marked within the Podil'tsi Fm. The Kokhanivka Fm. from the Korolyn 6, and Bortyatin 1 boreholes contains molecular traces of cyanobacteria.
3. Amongst terrestrial plants, traces of conifers, bryophytes, and fungi were marked. The samples from the Podil'tsi Fm. contain aliphatic oleanane, which in the Lower Jurassic might be linked, for example with Bennettitales. The Middle Jurassic strata are characterised by the absence of aliphatic diterpenoids, suggesting a low significance of conifers in the sediment supply area.
4. The Podil'tsi Fm. was deposited in dysoxic conditions in a sulphate-poor marine palaeoenvironment. The deposition of the Kokhanivka Fm. took place under suboxic redox conditions in a sulphate-poor fluvial–deltaic palaeoenvironment. Photic zone anoxia were observed within the Podil'tsi Fm.
5. Chemostratigraphic correlation with the Polish Basin allows the division of the Kokhanivka Fm. into three parts: lower, middle, and upper related to the Toarcian–Lower Aalenian, Middle–Upper Aalenian, and Bajocian–Bathonian Ages, respectively. The Medenychi Fm. is equivalent to the lower part of the Kokhanivka Fm.
6. The Podil'tsi and most of the Kokhanivka Fm. are characterised by poor hydrocarbon potential. Only the middle part of the Kokhanivka Fm. is characterised by fair-to-good hydrocarbon potential.

Supplementary Information The online version contains supplementary material available at https://doi.org/10.1007/s00531-023-02311-8.

Acknowledgements The results came from statutory work of AGH-University of Science and Technology, Faculty of Geology, Geophysics, and Environmental Protection nos. 16.16.140.315. The authors thank Prof. Ulrich Riller, Prof. Tadeusz Peryt, and one anonymous reviewer for their useful comments, which allowed us to improve this paper and had a significant contribution to the final version.

Data availability All Rock-Eval raw data obtained here are listed in Online Appendix 1. The raw files with chromatograms are not available. The rest of the data i.e. thin sections are available upon request.

Declarations

Conflict of interests The authors declare that they have no known competing financial interests or personal relationships that could have appeared to influence the work reported in this paper.

References

Ahmed M, George SC (2004) Changes in the molecular composition of crude oils during their preparation for GC and GC–MS analyses. Org Geochem 35:137–155. https://doi.org/10.1016/j.orggeochem.2003.10.002

Alexander R, Cumbers KM, Kagi RI (1986) Alkylbiphenyls in ancient sediments and petroleum. Org Geochem 10:841–845. https://doi.org/10.1016/S0146-6380(86)80021-3

Bray EE, Evans ED (1961) Distribution of n-paraffins as a clue to recognition of source beds. Geochim Cosmochim Acta 22:2–15. https://doi.org/10.1016/0016-7037(61)90069-2

Brocks JJ, Schaeffer P (2008) Okenane, a biomarker for purple sulfur bacteria (Chromatiaceae), and other new carotenoid derivatives from the 1, 640 Ma Barney Creek Formation. Geochim Cosmochim Acta 72:1396–1414. https://doi.org/10.1016/j.gca.2007.12.006

Brooks JD (1970) The use of coals as indicators of the occurrence of oil and gas. Australian Petrol Prod Explor Assoc J 10:35–40. https://doi.org/10.1071/AJ69007

Buła Z, Habryn R (2011) Precambrian and Palaeozoic basement of the Carpathian foredeep and the adjacent Outer Carpathians (SE Poland and western Ukraine). Ann Soc Geol Pol 81:221–239

Cesar J, Grice K (2019) Molecular fingerprint from plant biomarkers in Triassic-Jurassic petroleum source rocks from the Dampier sub-Basin, Northwest Shelf of Australia. Mar Pet Geol 110:189–197. https://doi.org/10.1016/j.marpetgeo.2019.07.024

Chen X, Liu X, Lin D, Wang J, Chen L, Yu P, Wang L, Xiong Z, Chen M (2021) A potential suite of climate markers of long-chain n-alkanes and alkenones preserved in the top sediments from the Pacific sector of the Southern Ocean. Prog Earth Planet Sci 8:23. https://doi.org/10.1186/s40645-021-00416-9

Cui X, Liu X-L, Shen G, Ma J, Husain F, Rocher D, Zumberge JE, Bryant DA, Summons RE (2020) Niche expansion for phototrophic sulfur bacteria at the Proterozoic-Phanerozoic transition. Proc Natl Acad Sci 117(30):17599–17606. https://doi.org/10.1073/pnas.2006379117

de Leeuw JW, Sinninghe-Damste JS (1990) Organic sulphur compounds and other biomarkers as indicators of palaeosalinity. In: Orr WL, White CM (Eds.), Geochemistry of Sulfur in Fossil Fuels. American Chemical Society, Washington, pp. 417–443. https://doi.org/10.1021/bk-1990-0429.ch024

Demaison G, Holck AJJ, Jones RW, Moore GT (1983) Predictive source bed stratigraphy; a guide to regional petroleum occurrence. In: Proceedings of the 11th World Petroleum Congress, Vol. 2, John Wiley & Sons, London, pp. 1–13

Didyk BM, Simoneit BRT, Brassell SC, Eglinton G (1978) Organic geochemical indicators of palaeoenvironmental conditions of sedimentation. Nature 272:216–222. https://doi.org/10.1038/272216a0

Dulub WG, Zhabina NM, Ogorodnik ME, Smirnov SE (2003) Poyasniuvalna zapiska do stratigrafichnoy skhemi yurskikh vikladiv Predkarpa'tia (Striyskii yurskii basein). Lvivske Viddilennia Ukrainskogo Derzhavnogo Geologorozviduvalnogo Instytutu, 30 p (in Ukrainian)

Ellis L (1994) Aromatic hydrocarbons in crude oils and sediments. PhD dis., Curtin Univ, of Technology, USA

Espitalié J, Laporte JL, Madec M, Marquis F, Leplat P, Paulet J, Boutefeu A (1977) Methode rapide de caracterisation des roches meres, de leur potential petrolier et de leur degree d'evolution. Revue Institute Francais Petrol 32:23–42. https://doi.org/10.2516/ogst:1977002

Fabiańska M (2007) Organic geochemistry of brown coals from the selected Polish basins: Wydawnictwo Uniwersytetu Śląskiego, Poland, 315 p. (In Polish, with English summary)

Feldman-Olszewska A (1997) Depositional architecture of the Polish epicontinental Middle Jurassic basin. Geol Quarterly 41:491–508

Ficken KJ, Li B, Swain DL, Eglinton G (2000) An *n*-alkane proxy for the sedimentary input of submerged/floating freshwater aquatic macrophytes. Org Geochem 31:745–749. https://doi.org/10.1016/S0146-6380(00)00081-4

Fowler MG, Douglas AG (1987) Saturated hydrocarbon biomarkers in oils of Late Precambrian age from Eastern Siberia. Org Geochem 11:201–213. https://doi.org/10.1016/0146-6380(87)90023-4

Gareckij RG (ed.) (1985) Sedimentation and palaeogeography of the western part of East European Platform in Mesozoic time. IUGS UNESCO, Project No. 86, Nauka i Tekhnika: Minsk: 211 pp (in Russian)

Goossens H, de Leeuw JW, Schenck PA, Brassell SC (1984) Tocopherols as likely precursors of pristane in ancient sediments and crude oils. Nature 312:440–442. https://doi.org/10.1038/312440a0

Grice K, Nabbefeld B, Maslen E (2007) Source and significance of selected polycyclic aromatic hydrocarbons in sediments (Hovea-3 well, Perth Basin, Western Australia) spanning the Permian-Triassic boundary. Org Geochem 38:1795–1803. https://doi.org/10.1016/j.orggeochem.2007.07.001

Gutowski J, Popadyuk IV, Olszewska B (2005) Late Jurassic-Earliest Cretaceous evolution of the epicontinental sedimentary basin of south-eastern Poland and Western Ukraine. Geol Quarterly 49:31–44

Hautevelle Y, Michels R, Malartre F, Trouiller A (2006) Vascular plant biomarkers as proxies for palaeoflora and palaeoclimatic changes at the Dogger/Malm transition of the Paris Basin (France). Org Geochem 37:610–625. https://doi.org/10.1016/j.orggeochem.2005.12.010

Huang WY, Meinschein WG (1979) Sterols as ecological indicators. In: Satyana AH (Ed.), Petroleum Geochemistry, Pre-Convention Short Course IAGI, Bandung. https://doi.org/10.1016/0016-7037(79)90257-6

Izart A, Palhol F, Gleixner G, Elie M, Blaise T, Suarez-Ruiz I, Sachsenhofer RF, Privalov VA, Panova EA (2012) Palaeoclimate reconstruction from biomarker geochemistry and stable isotopes of n-alkanes from Carboniferous and Early Permian humic coals and limnic sediments in western and eastern Europe. Org Geochem 43:125–149. https://doi.org/10.1016/j.orggeochem.2011.10.004

Karp AT, Holman AI, Hopper P, Grice K, Freeman KH (2020) Fire distinguishers: Refined interpretations of polycyclic aromatic hydrocarbons for paleo-applications. Geochim Cosmochim Acta 289:93–113. https://doi.org/10.1016/j.gca.2020.08.024

Karpenchuk Y, Zhabina N, Anikeyeva O (2006) Features and a structure and prospects for oil and gas presence in the Upper Jurassic reef complex in the Bilche-Volytsa outer zone of the Carpathian Foredeep. Geologiya i Geoklimiya Horyuchykh Kopalyn 2:44–52

Klomp UC (1986) The chemical structure of a pronounced series of iso-alkanes in South Oman crudes. Org Geochem 10:807–814. https://doi.org/10.1016/S0146-6380(86)80017-1

Koopmans MP, Rijpstra WIC, Klapwijk MM et al (1999) A thermal and chemical degradation approach to decipher pristane and phytane precursors in sedimentary organic matter. Org Geochem 30:1089–1104. https://doi.org/10.1016/S0146-6380(99)00088-1

Kosakowski P, Więcław D, Kowalski A, Koltun YV (2012) Assessment of hydrocarbon potential of Jurassic and Cretaceous source rocks in the Tarnogród-Stryi area (SE Poland and W Ukraine). Geol Carpath 63:319–333. https://doi.org/10.2478/v10096-012-0025-3

Kotarba MJ, Więcław D, Kosakowski P, Koltun YV, Kowalski A (2011a) Evaluation of hydrocarbon potential of the autochtonous Miocene strata in the NW part of the Ukrainian Carpathian Foredeep. Ann Soc Geol Pol 81:395–407

Kotarba MJ, Więcław D, Kosakowski P, Wróbel M, Matyszkiewicz J, Buła Z, Krajewski M, Koltun YV, Tarkowski J (2011b) Petroleum systems in the Palaeozoic-Mesozoic basement of the Polish and Ukrainian parts of the Carpathian Foredeep. Ann Soc Geol Pol 81:487–522

Krajewski M, Król K, Olszewska B, Felisiak I, Skwarczek M (2011) Facies of the Upper Jurassic-Lower Cretaceous sediments in the basement of the Carpathian Foredeep (western Ukraine). Ann Soc Geol Pol 81:291–307

Krajewski M, Ferré B, Salamon MA (2020) Cyrtocrinids (Cyrtocrinida, Crinoidea) and other associated crinoids from the Jurassic (Kimmeridgian–Tithonian)–Cretaceous (Berriasian–Barremian) of the Carpathian Foredeep basement (western Ukraine). Geobios 60:61–77. https://doi.org/10.1016/j.geobios.2020.04.005

Kurovets I, Prytulka H, Shyra A, Shuflyak Y, Peryt TM (2011) Petrophysical properties of the pre-Miocene rocks of the Outer Zone of the Ukrainian Carpathian Foredeep. Ann Soc Geol Pol 81:363–373

Marek S, Pajchlowa M, (eds.) (1997) The epicontinental Permian and Mesozoic in Poland. Prace Państwowego Instytutu Geologicznego 153. (In Polish with English summary)

Marynowski L, Simoneit BRT (2009) Widespread upper Triassic to lower Jurassic wildfire records from Poland: evidence from charcoal and pyrolytic polycyclic aromatic hydrocarbons. Palaios 24:785–798. https://doi.org/10.2110/palo.2009.p09-044r

Marynowski L, Smolarek J, Bechtel A, Philippe M, Kurkiewicz S, Simoneit BRT (2013) Perylene as an indicator of conifer fossil wood degrading by wood-degrading fungi. Org Geochem 59:143–151. https://doi.org/10.1016/j.orggeochem.2013.04.006

Marynowski L, Smolarek J, Hautevelle Y (2015) Perylene degradation during gradual onset of organic matter maturation. Int J Coal Geol 139:17–25. https://doi.org/10.1016/j.coal.2014.04.013

Mead R, Xu YP, Chong J (2005) Sediment and soil organic matter source assessment as revealed by the molecular distribution and

carbon isotopic composition of n-alkanes. Org Geochem 36:363–370. https://doi.org/10.1016/j.orggeochem.2004.10.003
Moldowan JM, Seifert WK, Gallegos EJ (1985) Relationship between petroleum composition and depositional environment of petroleum source rocks. Am Asso Petrol Geol Bull 69:1255–1268. https://doi.org/10.1306/AD462BC8-16F7-11D7-8645000102C1865D
Moldowan JM, Dahl J, Huizinga BJ et al (1994) The molecular fossil record of oleanane and its relation to angiosperms. Science 265:768–771. https://doi.org/10.1126/science.265.5173.768
Obermajer M, Fowler MG, Snowdon LR, Macqueen RW (2000) Compositional variability of crude oils and source kerogen in the Silurian carbonate-evaporite sequences of the eastern Michigan Basin, Ontario, Canada. Bull Can Pet Geol 48:307–322. https://doi.org/10.2113/48.4.307
Olszewska B, Matyszkiewicz J, Król K, Krajewski M (2012) Correlation of the Upper Jurassic-Cretaceous epicontinental sediments in southern Poland and southwestern Ukraine based on thin sections. Biuletyn Państwowego Instytutu Geologicznego 453:29–80
Otto A, Simoneit BRT (2002) Biomarkers of holocene buried conifer logs from Bella Coola and north Vancouver. British Columbia Canada Organ Geochem 33:1241–1251. https://doi.org/10.1016/S0146-6380(02)00139-0
Ovcharenko YK, Dulub VG, Burova MI, Karpenchuk YR (1999) Komarnian suite as a new element of Jurassic section at external flank of the Fore-Carpathian Depression. Geologiia i Geokhimiia Goriuchikh Kopalin 106:13–20 (**(in Ukrainian)**)
Pancost RD, Baas M, van Geel B, Sinninghe Damste JS (2002) Biomarkers proxies for plant inputs to peats: an example from a subboreal ombrotrophic bog. Org Geochem 22:675–690. https://doi.org/10.1016/S0146-6380(02)00048-7
Peters KE (1986) Guidelines for evaluating petroleum source rock using programmed pyrolysis. Am Asso Petrol Geol Bull 70:318–329. https://doi.org/10.1306/94885688-1704-11D7-8645000102C1865D
Peters KE, Cassa MR (1994) Applied source rock geochemistry. In: Magoon LB, Dow WG (eds.) The Petroleum System – From Source to Trap, American Association of Petroleum Geologists, Tulsa, OK pp. 93–117. https://doi.org/10.1306/M60585C5
Peters KE, Moldowan JM (1993) The Biomarker Guide: Interpreting Molecular Fossils in Petroleum and Ancient Sediments. Englewood Cliffs, N. J.
Peters KE, Walters CC, Moldowan JM (2005) The Biomarker Guide Vol. 2, 2nd ed, Cambridge University Press, Cambridge, UK
Philp P, Wood M, Gorenekli YS, Nguyen T, Symcox C, Wang H, Kim D (2021) The presence of 18a(H)-oleanane in Pennsylvanian and Mississippian rocks in the Anadarko Basin, Oklahoma. Organ Geochem 152:104181. https://doi.org/10.1016/j.orggeochem.2021.104181
Pieńkowski G (2004) The epicontinental Lower Jurassic of Poland. Polish Geological Institute, Special Papers 12:1–122
Popa ME, Zaharia A (2011) Early Jurassic ovipositories on bennettitalean leaves from Romania. Acta Palaeontologica Romaniae 7:285–290
Rauball JF, Sachsenhofer RF, Bechtel A (2020) Petroleum potential of Middle Jurassic rocks in the basement of the Carpathian Foredeep (Ukraine) and oil-to-source correlation with oil in Upper Jurassic reservoirs. Geologica Carpathica 71(2): 150–165. https://doi.org/10.31577/GeolCarp.71.2.4
Romero-Sarmiento MF, Riboulleau A, Vecoli M, Laggoun-Défarge F, Versteegh GJM (2011) Aliphatic and aromatic biomarkers from Carboniferous coal deposits at Dunbar (East Lothian, Scotland): Palaeobotanical and palaeoenvironmental significance. Palaeogeogr Palaeoclimatol Palaeoecol 309:309–326. https://doi.org/10.1016/j.palaeo.2011.06.015
Ruebsam W, Pieńkowski G, Schwark L (2020) Toarcian climate and carbon cycle perturbations – its impact on sea-level changes, enhanced mobilization and oxidation of fossil organic matter. Earth Planet Sci Lett 546:116417. https://doi.org/10.1016/j.epsl.2020.116417
Schwark L, Frimmel A (2004) Chemostratigraphy of the Posidonia black shale, SW Germany: II. Assessment of extent and persistence of photic-zone anoxia using aryl isoprenoid distributions. Chem Geol 206:231–248. https://doi.org/10.1016/j.chemgeo.2003.12.008
Seifert WK, Moldowan JM (1979) The effect of biodegradation on steranes and terpanes in crude oils. Geochim Cosmochim Acta 43:111–126. https://doi.org/10.1016/0016-7037(79)90051-6
Shanmugam G (1985) Significance of coniferous rain forests and related organic matter in generating commercial quantities of oil, Gippsland Basin, Australia. Am Asso Petrol Geol Bull 69:1241–1254. https://doi.org/10.1306/AD462BC3-16F7-11D7-8645000102C1865D
Shiea J, Brassell SC, Ward DM (1990) Mid-chain branched mono- and dimethyl alkanes in hot spring cyanobacterial mats: a direct biogenic source for branched alkanes in ancient sediments? Org Geochem 15:223–231. https://doi.org/10.1016/0146-6380(90)90001-G
Silva Souza IM, Zambrano ERN, de Souza ES, Parra CJO, Severiano Ribeiro HJP, Cerqueira JR, Mortatti J, de Oliveira OMC, de Souza Queiroz AF (2022) Biomarkers and PAH chemostratigraphy in the study of the Frasnian anoxic event in the Pimenteiras Formation outcrop of the Parnaíba Basin, Brazil. Palaeogeography Palaeoclimatol Palaeoecol 598:111033. https://doi.org/10.1016/j.palaeo.2022.111033
Simoneit BRT (1977) Diterpenoid compounds and other lipids in deep-sea sediments and their geochemical significance. Geochim Cosmochim Acta 41:463–476. https://doi.org/10.1016/0016-7037(77)90285-X
Simoneit BRT (2005) A review of current applications of mass spectrometry for biomarker/molecular tracer elucidations. Mass Spectrometry Rev 24(5):719–765. https://doi.org/10.1002/mas.20036
Sinninghe Damsté JS, Kenig F, Koopmans MP, Köster J, Schouten S, Hayes JM, de Leeuw JW (1995) Evidence for gammacerane as an indicator of water column stratification. Geochim Cosmochim Acta 59:1895–1900. https://doi.org/10.1016/0016-7037(95)00073-9
Slatt RM, Zhang J, Torres-Parada E, Brito R, Duarte D, Milad B (2021) Unconventional Petroleum Resources. In: Alderton D, Elias SA (eds) Encyclopedia of Geology, 2nd edn. Academic Press, pp 783–807
Song J, Littke R, Weniger P (2017) Organic geochemistry of the Lower Toarcian Posidonia Shale in NW Europe. Org Geochem 106:76–92. https://doi.org/10.1016/j.orggeochem.2016.10.014
Świdrowska J, Hakenberg M, Poluhtović B, Seghedi A, Višnikov I (2008) Evolution of the Mesozoic Basins on the south western edge of the East European Craton (Poland, Ukraine, Moldova, Romania). Studia Geologica Polonica 130:3–130
Taylor DW, Li H, Dahl J, Fago FJ, Zinniker D, Moldowan JM (2006) Biogeochemical evidence for the presence of the angiosperm molecular fossil oleanane in paleozoic and mesozoic non-angiospermous fossils. Paleobiology 32(2):179–190. https://doi.org/10.1666/0094-8373(2006)32[179:BEFTPO]2.0.CO;2
Ten Haven HL, de Leeuw JW, Rullkötter J, Sinninghe Damsté JS (1987) Restricted utility of the pristane/phytane ratio as a palaeoenvironmental indicator. Nature 330:641–643. https://doi.org/10.1038/330641a0
Van Aarssen BGK, Alexander R, Kagi RI (2000) Higher plant biomarkers reflect palaeovegetation changes during Jurassic times. Geochim Cosmochim Acta 64:1417–1424. https://doi.org/10.1016/S0016-7037(99)00432-9

Varnosfaderany MN, Bakhtiari AR, Gu Z, Chu G (2014) Perylene as an indicator of land-based plant biomarkers in the southwest Caspian Sea. Mar Pollut Bull 80:124–131. https://doi.org/10.1016/j.marpolbul.2014.01.033

Volkman JK (2003) Sterols in microorganisms. Appl Microbiol Biotechnol 60:495–506. https://doi.org/10.1007/s00253-002-1172-8

Wang X, Li M, Fang R, Lai H, Lu X, Liu X (2022) The distributions and geochemical implications of methylated 2-methyl-2-(4,8,12-trimethyltridecyl)chromans in immature sediments. Energy Explor Exploit 40(1):343–358. https://doi.org/10.1177/01445987211033342

Xu H, George SC, Hou D (2019) Algal-derived polycyclic aromatic hydrocarbons in Paleogene lacustrine sediments from the Dongying Depression, Bohai Bay Basin, China. Mar Pet Geol 102:402–425. https://doi.org/10.1016/j.marpetgeo.2019.01.004

Yunker MB, Macdonald RW, Vingarzan R, Mitchell RH, Goyette D, Sylvestre S (2002) PAHs in the Fraser River basin: A critical appraisal of PAH ratios as indicators of PAH source and composition. Org Geochem 33:489–515. https://doi.org/10.1016/S0146-6380(02)00002-5

Zakrzewski A, Kosakowski P (2021) Impact of palaeo-wildfires on higher plant parameter revealed by new biomarker indicator. Palaeogeography Palaeoclimatol Palaeoecol 579:110606. https://doi.org/10.1016/j.palaeo.2021.110606

Zakrzewski A, Kosakowski P, Waliczek M, Kowalski A (2020) Polycyclic aromatic hydrocarbons in Middle Jurassic sediments of the Polish Basin as evidence of high-temperature palaeo-wildfires. Organ Geochem 145:104037. https://doi.org/10.1016/j.orggeochem.2020.104037

Zakrzewski A, Waliczek M, Kosakowski P (2022a) Geochemical and petrological characteristics of the Middle Jurassic organic-rich siliciclastic sediments from the central part of the Polish Basin. Int J Coal Geol 255:103986. https://doi.org/10.1016/j.coal.2022.103986

Zakrzewski A, Waliczek M, Kosakowski P, Pańczak J (2022b) Lower Jurassic in the central part of the Polish Basin - geochemical and petrological approach. Marine Petrol Geol 146:105922. https://doi.org/10.1016/j.marpetgeo.2022.105922

Zhabina NM, Anikeyeva OV (2007) Onovlena stratigrafichna skhema verkhnoy yury–neokomu ukrainskogo Peredkarpattya. Zbirnik Naukovykh Prac 3:46–56 (**(in Ukrainian)**)

Zhabina NM, Shlapinsky VY, Prykhodko MG, Anikeyeva OV, Machalsky DV (2017) The generalizated stratigraphic scheme of the Jurassic of Western Ukraine. Geol J 4:9–22

Ziegler PA (1990) Geological atlas of western and central Europe. Shell Internationale Petroleum Maatschappij BV, The Hague